OF 84-15
CHARACTERIZATION OF ALASKAN COALS: EVALUATION OF THEIR LIQUEFACTION BEHAVIOR

FINAL TECHNICAL PROGRESS REPORT

By
J.S. Youtcheff and P.D. Rao
July, 1984 - February, 1986

CHARACTERIZATION OF ALASKAN COALS:

EVALUATION OF THEIR LIQUEFACTION BEHAVIOR

Final Technical Progress Report
July, 1984 - February, 1986

J.S. Youtcheff and P.D. Rao

Mineral Industry Research Laboratory
University of Alaska-Fairbanks
Fairbanks, Alaska 99775-1180

Prepared for:

The United States Department of Energy
Under Contract DE-FG22-84PC70774

ABSTRACT

Nineteen coals, representing seven of Alaska's coal fields, were liquefied in batch reactors at 425°C with tetralin as the donor solvent. The lignite and subbituminous coals from Little Tonzona, Nenana, Beluga and Yukon Flats coal fields were found to readily convert to THF solubles plus gases. Conversions for these coals were greater than 84% (daf basis). The bituminous coal from the Matanuska coal field and the inertinite-rich coals from the Northern Alaska and Chicago Creek coal fields were considerably less reactive; conversion yields from 55 to 82 % were attained. A number of correlations were examined between conversion yield and coal characteristics.

Evaluation of the distribution of liquefaction products showed that the low rank coals are readily converted into low molecular weight components (oils plus gases) and few asphaltenes and preasphaltenes. The inertinite rich and other less reactive coals produced equal distributions of the three product classes.

The coals and hexane-insolubles were analyzed using DRIFT spectroscopy. The spectrum of HZA was found to be similar to that of a guaiacyl-type lignin. Changes in the spectral features as a function of liquefaction severity were examined.

Preliminary studies were conducted to enhance an understanding of fluorescent vitrinite, inertinite macerals and the role of cations during liquefaction. The primary fluorescence exhibited by the ulminite in the HZA coal appears to be attributed to the presence of substituted aromatics. Some of the inertinites in UA-139 were determined to be reactive. The presence of cations was found to

enhance the conversion of UCM-11 and CSB-13, presumably by diminishing the tendency for condensation reactions to occur.

TABLE OF CONTENTS

LIST OF FIGURES

LIST OF FIGURES (continued)

LIST OF TABLES

ACKNOWLEDGMENTS

The authors would like to thank Jane Smith for her technical assistance with the Petrographic analyses. We would like to acknowledge Sang-Ho Lee and Suresh Paranjpe, the two graduate students who worked on a number of tasks in this project. Special thanks go to Cathy Farmer who typed this report.

This work was conducted with funds provided by the U.S. Department of Energy under grant DE-FG22-84PC70774. Additional support was provided by a special Alaska state appropriation through a grant to the Mineral Industry Research Laboratory.

I. INTRODUCTION

Alaska's coal resources are of Cretaceous and Tertiary age. Most of the Cretaceous coals are located in Northern Alaska. Estimates of hypothetical resources for northern Alaska coals are on the order of several trillion tons. These coals range in rank from subbituminous A to high volatile A bituminous. The impediments to exploitation of these vast resources are twofold:

1. The continental shelves of the Bering and Chuckchi seas give rise to fairly shallow water on the north western coasts; it is necessary to go three miles or more from shore in order to find water depths of sixty feet.
2. The shipping season without the aid of ice breakers is limited to 3 months a year.

Conversion of these coals to clean liquid fuels and their subsequent transport via pipeline to an ice-free port may prove to be the best way to utilize the coal resources of northern Alaska.

In central and southern Alaska large resources of subbituminous C rank coals have been identified. Their conversion to liquid fuels would enhance their marketability in the western United States and in Pacific Rim Countries.

An additional consideration, which makes the liquefaction of Alaskan coals attractive, is that the State has estimated recoverable reserves of 150 - 200 trillion cu. ft. of natural gas. The steam reforming of methane may be a viable source of hydrogen for coal liquefaction processes.

Mechanism of Coal Liquefaction

Coal liquefaction is quite complex and subject to much speculation. As the coal matrix is heated, thermal ruptures of labile bonds result. This breakdown of the macromolecular structure is quite variable. It is dependent on the number and type of bonds involved in cross-linking the structure, the type of soluble components generated upon cleavage of these linkages, the demand for hydrogen to stabilize the generated radicals, and the penetrability of the coal matrix by the donor solvent. Initially the generated free radicals are capped by hydrogen transferred from hydroaromatic systems within the coal. These systems are most likely extractable from mobile molecules. Once the coal matrix is sufficiently comminuted or opened up, the donor solvent is able to penetrate the coal particles and becomes involved in capping the free radicals. The key to optimum liquefaction of the coal appears to be centered around the early stages of liquefaction, where internal hydrogen transfer is operating. The amount and availability of these species appears to be rank dependent. For example, in the event where insufficient amounts of internal hydrogen exists such as in low rank coals, conversion is affected by the ability of the solvent to rapidly solubilize material and prevent coalescence or agglomeration of the particles (Derbyshire, 1982).

Due to the various biological sources and geological environments involved in the formation of coal, the nature and behavior of coals under different processing environments are quite varied. During the past few years a considerable effort has been made towards the correlation of coal characteristics with liquefaction behavior. These

studies were primarily based on ultimate, proximate and petrographic analyses. Correlations have been made between conversion (usually defined by solvation yield) and reactive maceral content (Given et al., 1975b), as well as with VM, carbon content, and H/C ratio (Given et al., 1980; Gray et al., 1980; Durie, 1980; Epperly, 1980). Although similar correlations have been seen for a wide range of coals, the ranking of the different factors will vary from seam to seam. For instance coals of similar rank but varying geological provinces have been shown to differ in behavior and chemical composition (Yarzab et al., 1979). One of the variations they reported was that the fraction of O as OH in coal showed a province dependence. Hence it is difficult to predict the liquefaction behavior of Alaskan coals in light of what is known concerning the coals of the conterminous United States, since these established empirical correlations may not apply.

The prime objective of this research was to further characterize Alaskan coal, and to evaluate the potential of these coals as feedstocks in direct liquefaction processes. A secondary goal was to initiate research activities which would enhance an understanding as to the chemistry and reactivity of inertinite macerals and fluorescent vitrinites.

II. PROCEDURES

1. Selection of Coal Samples

Extensive coal deposits are found throughout Alaska. Hypothetical resources are estimated at 4 trillion tons (Schaff, 1983). The major coal resource areas in the state are shown in Figure 1.

One of the objectives of this project is to gain a better understanding as to the potential of Alaskan coals as feedstocks in direct liquefaction processes. To this end a diverse group of coals representing seven of Alaska's coalfields was selected. A map indicating the location of these resource areas is shown in Figure 2. The ages and depositional environments for these coals are quite different. The coals from the Northern Alaska and Matanuska coal fields are Cretaceous in age, while the remainder of the set consists of Tertiary coals.

Nineteen coals were ultimately selected for this study. Six of the coals were taken from an in house sample bank. Nine samples were obtained from coal fields in which exploratory work is being conducted or was recently concluded. These coals were generally obtained from drill hole cores. The coals from Little Tonzona, Chicago Creek and Northern Alaska fall into this category. The remaining 4 samples were collected during the course of this project. For an indepth discussion on many of these coals see Rao and Wolff (1980; 1982) and Rao and Smith (1983).

In general these coals were chosen based on several criteria:

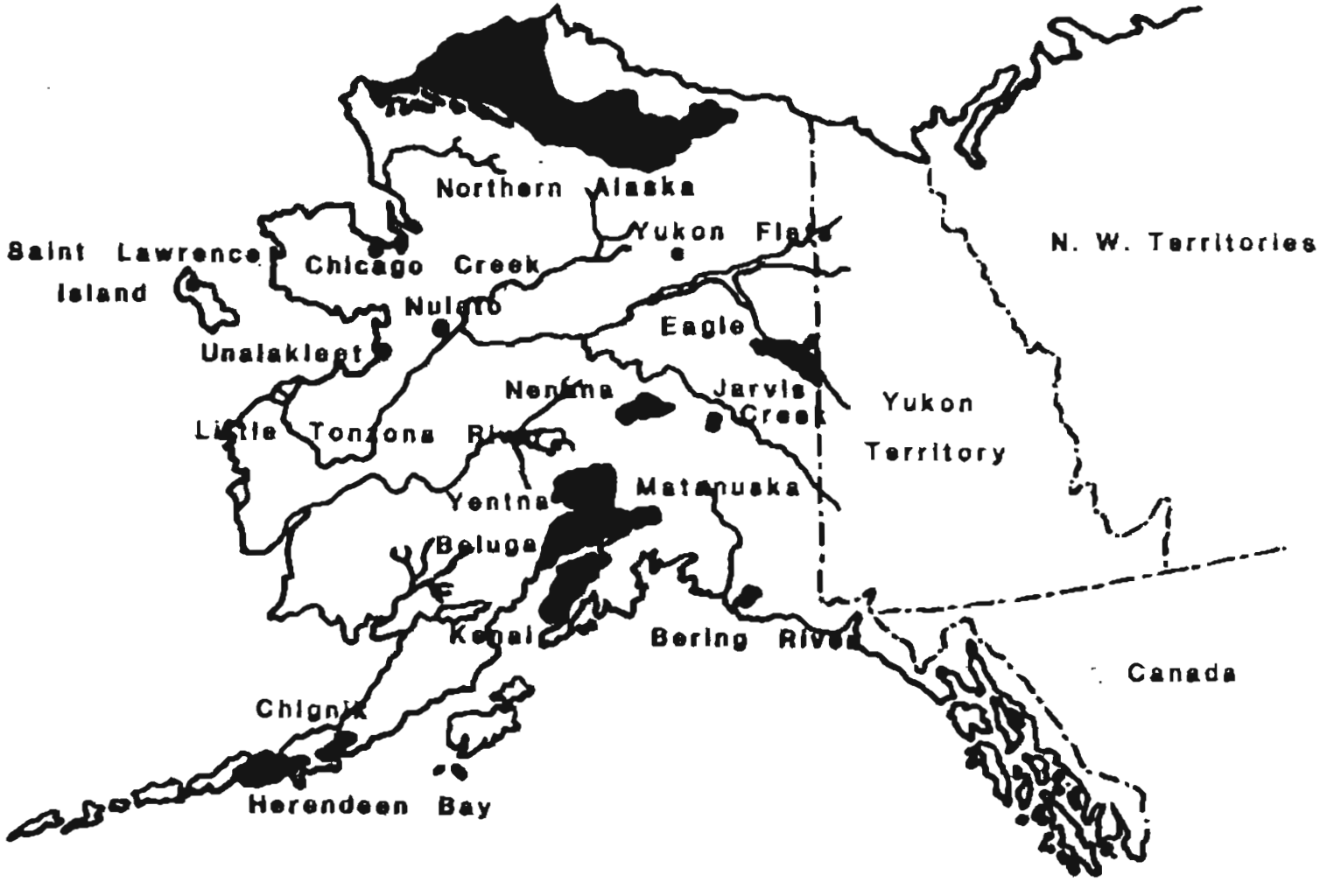

Figure 1: Major Coal Resource Areas in Alaska

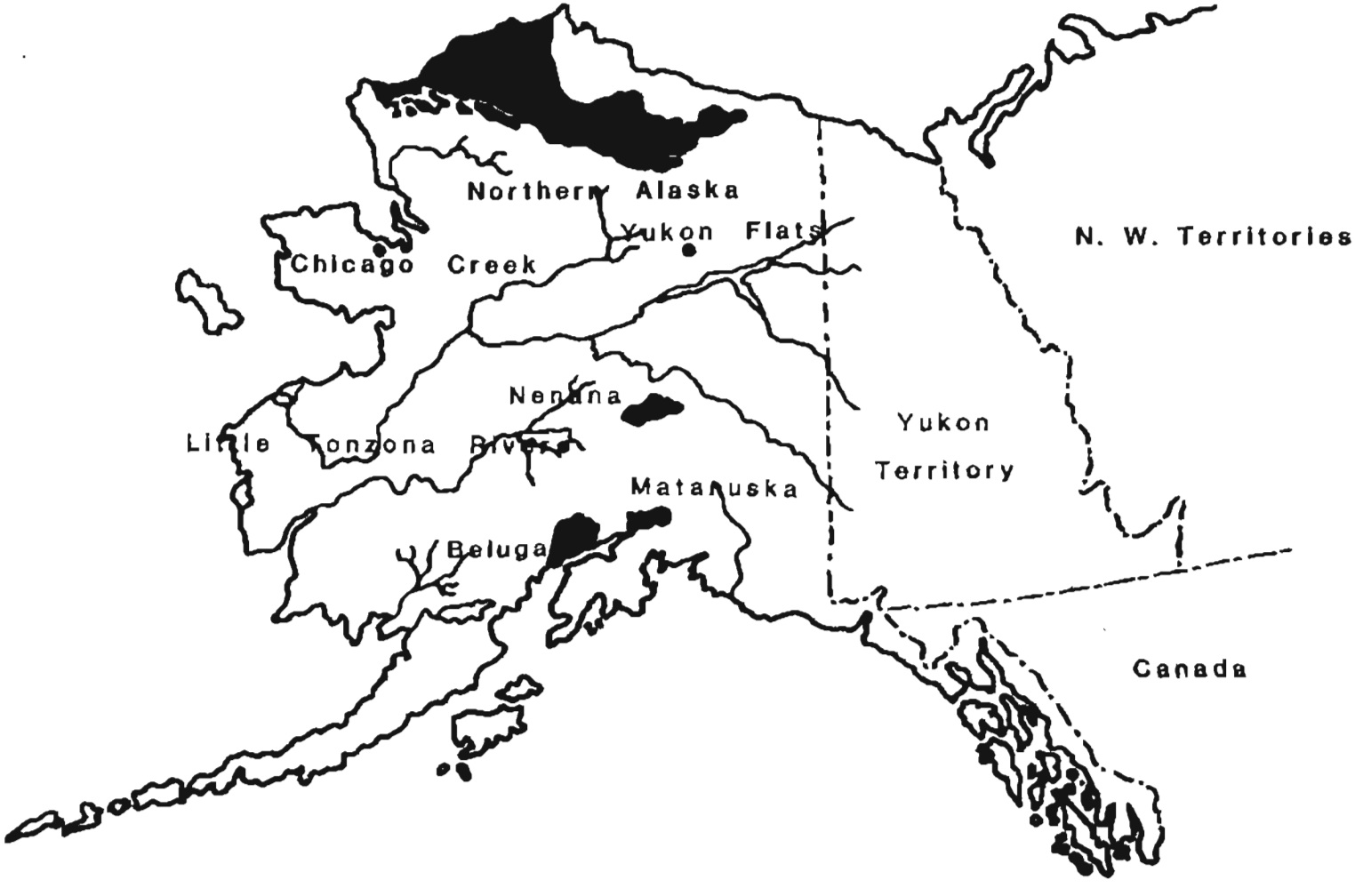

Figure 2: Coal Resource Areas Represented in Sample Set

1) that they had not been extensively oxidized; coals were obtained from freshly exposed beds or fresh exposures of previously mined beds;
2) that a wide range of coal rank was covered, or
3) that the coals are from coal fields of economical importance, that is, they are actively being mined, developed or considered for the near future.

Details regarding the sampling description and location of these coal samples are listed in Table 1.

Two surficial coals are included from the Yukon Flats; one of which the HZA coal was found to exhibit an anomalous behavior. Barker (1981) found this coal to produce a moderately hard coking button (FSI of 2). The principal investigator noted that this coal swells in the presence of THF or pyridine (unpublished results). This behavior exists despite the coal being classified as a subbituminous C coal (R_{om} of 0.25) and that these properties may have been distorted by weathering. The second coal was taken from the same vicinity. No atypical behavior has been observed for this coal.

Two field trips were undertaken (1 year apart) in order to locate the outcrop and source of this rubble, as well as to obtain fresh samples of the HZA coal. Although no outcrops were located, samples of the same coals were obtained on each occasion. The coal samples obtained consisted of both vitreous looking chunks of coal with concoidal fractures and weathered chunks of coal with rounded edges.

TABLE 1.

COAL FIELD	SAMPLE NUMBER	SEAM AND LOCATION	THICKNESS (FEET)	SAMPLE DESCRIPTION	ASTM RANK
Beluga	UA-148	Waterfall Bed	36	Channel Bench, top 6'	Subbit C
Chicago Creek	DH 1-2	Hole No. 1 (123-126.5)	107	Drill Core	Lignite
	DH 1-4	Hole No. 1 (141-150)		Drill Core	Lignite
	DH 1-5	Hole No. 1 (150-160)		Drill Core	Lignite
	DH 1-6	Hole No. 1 (160-170)		Drill Core	Lignite
Little Tonzona	CS-41730	Hole No. 3 (121-130.5)		Drill Core	Subbit C
	CS-41735	Hole No. 3 (351.5-357.5)		Drill Core	Subbit C
Matanuska	UA-107	Lower Seam, Castle Mountain	7	Channel	hvAb *
Nenana	UA-119	No. 4 Bed, Usibelli Mine	24	Channel	Subbit C
	UA-129	No. 1 Bed, Usibelli Mine	18	Channel	Subbit C
	UA-130	No. 3 Bed, Usibelli Mine	17	Channel	Subbit C
	2 UCM-11	No. 4 Bed, Usibelli Mine		Channel Bench, top 1'	subbit C
Northern Alaska	UA-139	No. 7 Bed, Cape Beaufort	17	Channel	hvCb *
	SS 67-1	Unnamed, Kukpowruk River	21	Channel bench, top 5'	hvAb
	SS 67-2	Unnamed, Kukpowruk River		Channel bench, Middle 5'	hvAb
	SS 67-3	Unnamed, Kukpowruk River		Channel bench, Lower 5'	hvAb
	CSB 13	No. 7 Bed, Cape Beaufort	17	Auger Hole	hvCb *
Yukon Flats	HZA			Rubble on gravel bar	Subbit C*
	HZE1			Rubble on gravel bar	Lignite *

* Apparent Rank

2. Characterization of Coals in the Sample Set

a) Rank Determinations

A number of coals (6) used in this study were taken from an in-house sample bank. High temperature ash analyses were determined for samples of these coals from new cans. Those samples whose ash content deviated significantly from that reported previously (Rao and Wolff, 1980; 1982) were characterized along with the new coal samples. Characterization included: ultimate and proximate analyses, calorific value determinations, and total sulfur determination.

b) Coal Petrology

Samples were crushed to -20 mesh and made into duplicate one-inch diameter pellets using an epoxy binder. Vitrinite reflectance measurements were determined following ASTM procedures. An Orthoplan microscope equipped with a MPV-3 photometry system, a peak reader and a motorized stage attachment was used to conduct this task.

Maceral analyses of the samples were done by point counting duplicate pellets. Normal incident light illumination was used when counting the huminite and inertinite macerals. The pellets were again counted using blue-light excitation for the fluorescent vitrinite and liptinite macerals.

Fluorescence spectra were generated on the Leitz Orthoplan microscope described above. This was equipped with a ploemopak fluorescence illuminator using filter block A3 for short-wave UV excitation. An 100W ultra-high pressure mercury lamp was used for the light source. The light was passed through a heat filter (BG23), an excitation filter (UG1), an interference beamsplitter (TK 400) and a

suppression filter (K430). A 63x fluorescence oil immersion objective was used for measuring purposes. A monochromator was used to spectrally disperse the fluorescent light from a range of 400 nm to 750 nm. The exit slit for the monochromator was set such that 3.3nm were allowed to pass at one time during the scan, and the photometer-measuring diaphragm which acts as the monochromator entrance slit is adjusted accordingly. A photomultiplier with an extended range for use with UV measurements (EMI 9558 with an S20 cathode) was used. All measurements were recorded on an HP85 Computer equipped with a fluorescence program package developed at E. Leitz, Inc. In order to measure the effects of alteration, or the change in fluorescent intensity with respect to irradiation time, the system was first standardized using a 100W tungsten halogen lamp as a reference. Correction factors were determined for each 10 nm interval, and were used to eliminate any effect caused by the apparatus.

c) Functional Group Determinations

Total carboxylates, ion exchanged carboxylates and hydroxyl contents were determined for the coals in the sample set. Hydroxyl determinations followed that of Szladow (1979). The hydroxyl groups were acetylated using acetic anydride in the presence of pyridine. After three days the reaction was quenched with water and the residual acetic acid was titrated with a standard solution of sodium hydroxide. This procedure enables the characterization of both alcoholic and phenolic hydroxyl groups. The one disadvantage of this method is that primary and secondary amines may be converted to amides during the course of the reaction.

Total carboxyl groups were determined by an ion exchange method using calcium acetate (Cronauer and Ruberto, 1977). The carboxylate salts are first converted to the acid form by treating the coal with 1N HCl at room temperature overnight. Roughly 250 mg of this treated coal is stirred with 10 ml of 1N calcium acetate and 50 ml of deionized water overnight at room temperature. The acetic acid liberated in the exchange is then titrated with standard NaOH solution using phenophthalein indicator.

Carboxylate groups were also determined utilizing ion exchange of ammonium ions as done by Morgan and others (1981). Approximately 0.5 gm were stirred with 50 ml of 1N ammonium acetate at room temperature for 3 hr. The solution was then filtered and washed with 25 ml of 1N ammonium acetate. This procedure was repeated 6 additional times. The filtrates were acidified with 5 ml of glacial acetic acid and analyzed for Ca, Mg, Na, K, Sr and Ba using a Specrometric Spectrospan V plasma emission spectrometer.

d) Major and Trace Elements

Major oxide and trace component analyses of the high temperature ash were determined by DC plasma emission spectrometry. Preparation of sample for analysis followed that of Suhr and Gong (1983). Approximately 200 mg of sample were fused with 1 gm lithium metaborate and dissolved in 100 ml 4% HNO_3. These solutions were used in the analysis of trace elements. The solution was further diluted with a diluent containing a 2000 μ gm/ml Li buffer.

3. Densimetric Fractionations

Float-sink separations were conducted on an air-dried sample of UA-139. The coal was crushed in a hammer mill to below 14 mesh particle size. Separations were then made at 1.3, 1.4 and 1.6 specific gravities using perchloroethylene-naphtha mixtures as the liquid density medium. Following this, the various fractions were crushed further to minus 60 mesh and characterized as per the parent coal.

4. Liquefaction Procedures

Batch liquefaction runs were conducted using an adaptation of the reactor system designed by Szladow (1979). Tubing bomb reactors were fabricated following the design of Youtcheff (1983).

The established procedure was to charge the tubing bombs with 2.5 gm of as received coal and 6 ml of tetralin. The microreactors were then leak checked and purged with nitrogen prior to pressurizing the reactors to 600 psig with hydrogen. The microreactors were mounted in a holder and connected to an oscillation device. They were then shaken for two minutes to effect the mixing of the coal and donor solvent. Liquefaction runs were initiated by immersing the reactors in a fluidized sand bath maintained at 425°C. It took two minutes for the reactors to achieve this reaction temperature. Upon conclusion of a run, the microreactors were immersed in cold water and allowed to equilibrate at room temperature for 0.5 hours.

The gases were vented and the contents of the reactors were quantitatively transferred to a 500-ml beaker. Hexane was used to effect the transfer. The recovered products were then transferred to

a 500-ml Erlenmeyer flask, diluted with hexane to 500-ml total volume, and left overnight to allow the hexane-insolubles to settle. The precipitate was collected by filtration on a 0.45μ Millipore filter and washed with 150 ml hexane. The filter cake was then dried in a vacuum oven at 100°C for 24 hours.

An aliquot of the hexane-insolubles was placed in a dried tared alundum crucible and exhaustively extracted for 24 hours in a Soxhlet apparatus with toluene under a nitrogen atmosphere. Following this, the extracted thimble was dried in a vacuum oven at 110°C for 12 hours and reweighed. The procedure was then repeated using tetrahydrofuran (THF). The material remaining in the crucible following extraction with THF is defined as the residue; this was also saved for analysis.

5. Characterization of the Liquefaction Products

Fourier Transform Infrared Spectroscopy (FTIR) was used to conduct gross structural examination of the coals and hexane insolubles. Analyses were conducted on a Digitlab Model FTS 15/B Fourier Transform Infrared Spectrometer at the Pennsylvania State University. The organic matrix of the coal and hexane-insolubles was examined using both absorption and diffuse reflectance modes. For the latter mode of operation, 5-10 mg of coal was ground with 300 mg of KBr in a Wig-L-Bug grinder. The dispersed sample was placed in a holder cup located where the incident light is focused onto the powder and the scatter light is collected using mirrors. Four hundred scans (Interferograms) of the sample at 2 cm^{-1} resolution were co-added to generate each spectrum of coal.

III. EXAMINATION OF COAL CHARACTERISTICS

Data regarding the characteristics of coals in the sample set are compiled in Appendix A. The diversity in the coals contained in this set is readily apparent when one considers the range of coal characteristics. Several of these are listed in Table 2.

Table 2. Range of Characteristics of Coals in Sample Set

Age ASTM Class	Cretaceous Lignite Minimum	Tertiary HVA Bituminous Maximum
% C, daf	63.40	85.52
% O, daf	6.07	29.61
% S, dry	.18	3.23
H/C	0.65	1.1
% Vitrinite	46.5	95.4
% Exinite	1.9	22.6
% Inertinite	2.6	40.0
Ro_{max}	0.16	0.98

Incorporated in this set are coals of Cretaceous and Tertiary Age which range in rank from lignite to HVA bituminous. Some of the coal properties, such as the vitrinite reflectance for the coals examined here, happen to partition by the age of the deposit. The Tertiary coals give rise to Ro_{max} classes between V_1 and V_5 and the Cretaceous coals have Ro_{max} classes ranging from V_5 through V_{11}. The highest R_{max} was found in the Matanuska coal (UA-107). This is largely due to the fact that the coals from this region have undergone thermal alterations due to igneous intrusions. Due to the nonmarine origin of these coals, the sulfur contents are quite low. Aside from the

Chicago Creek coals, total sulfur values are generally well below the 1% level on a dry ash free basis.

Petrographically there are large variations in this suite of coals. Those from the Nenana coal field are high in exinites, which range from 9.8% to 22.6% by volume on a mineral free basis. Most of the Northern Alaska and Chicago Creek coals contain an abundance of inertinite macerals; the inertinites range from 5.4% to 40% by volume (mmf). Most of these "inert" macerals were found to consist of low reflecting semifusinites. The Chicago Creek coals are classified as lignites. Despite this rank classification, many of their characteristics such as Ro_{max}, carbon content, calorific volume and volatile matter content suggest that these coals are more mature than the subbituminous coals from the Beluga and Nenana coal fields.

Even though there is a great diversity in characteristics and maceral composition of coals in this sample set, many properties correlate with each other. Carbon contents were found to correlate extremely well with both calorific value (Figure 3) and vitrinite reflectance Ro_{max} (Figure 4); correlation coefficients (R^2) for these relationships are .937 and .945, respectively. The coals from a particular basin were found to cluster around one another. Much of this is attributable to the diversity of rank and the variations in maceral composition for coals from a particular coal field as noted above.

The results of the analyses for oxygen functional groups are listed in Table 3. In a few cases the amount of carboxylates was found to exceed that of the total concentration of carboxyl groups.

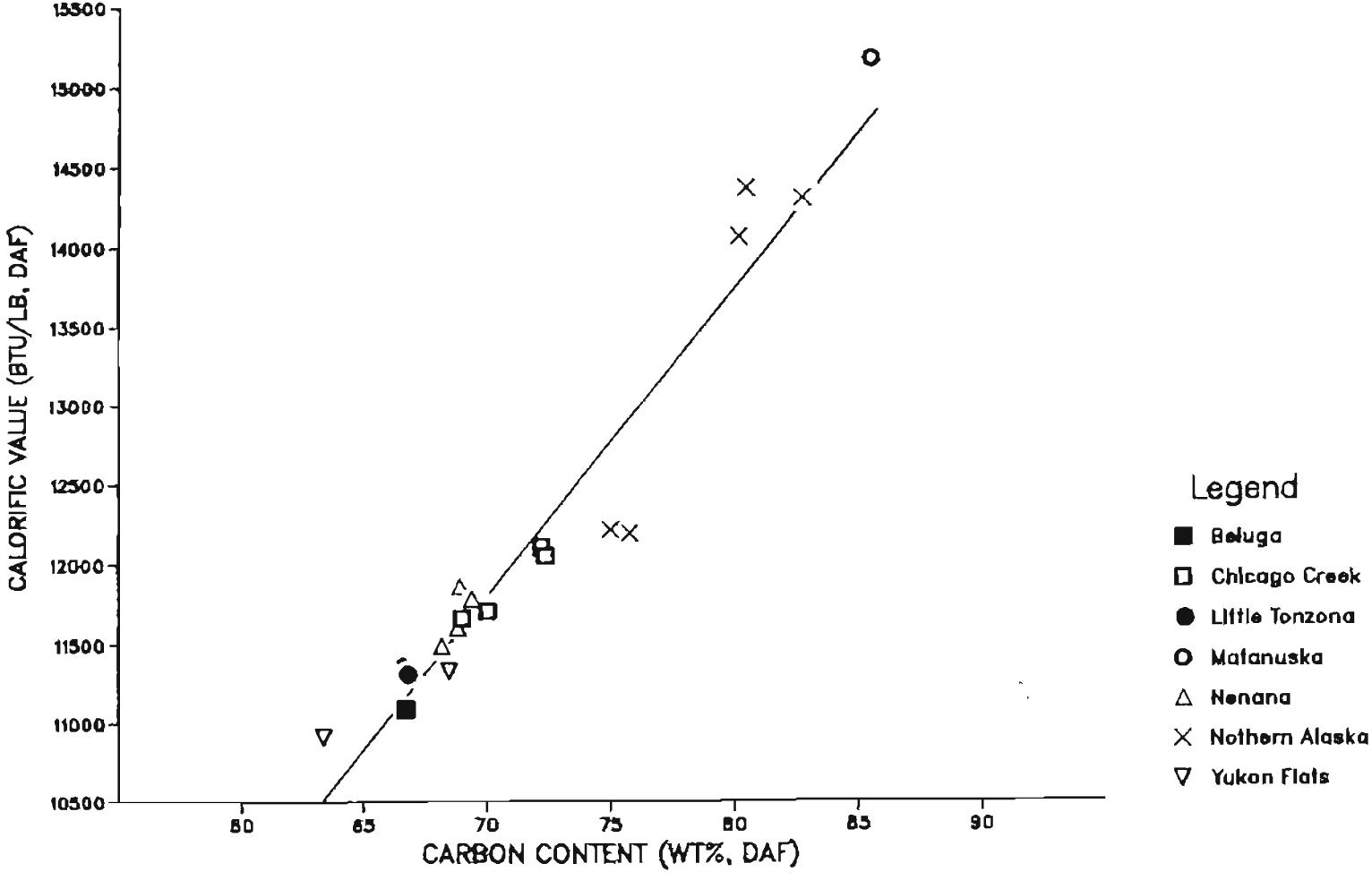

Figure 3. Correlation of calorific value with carbon content.

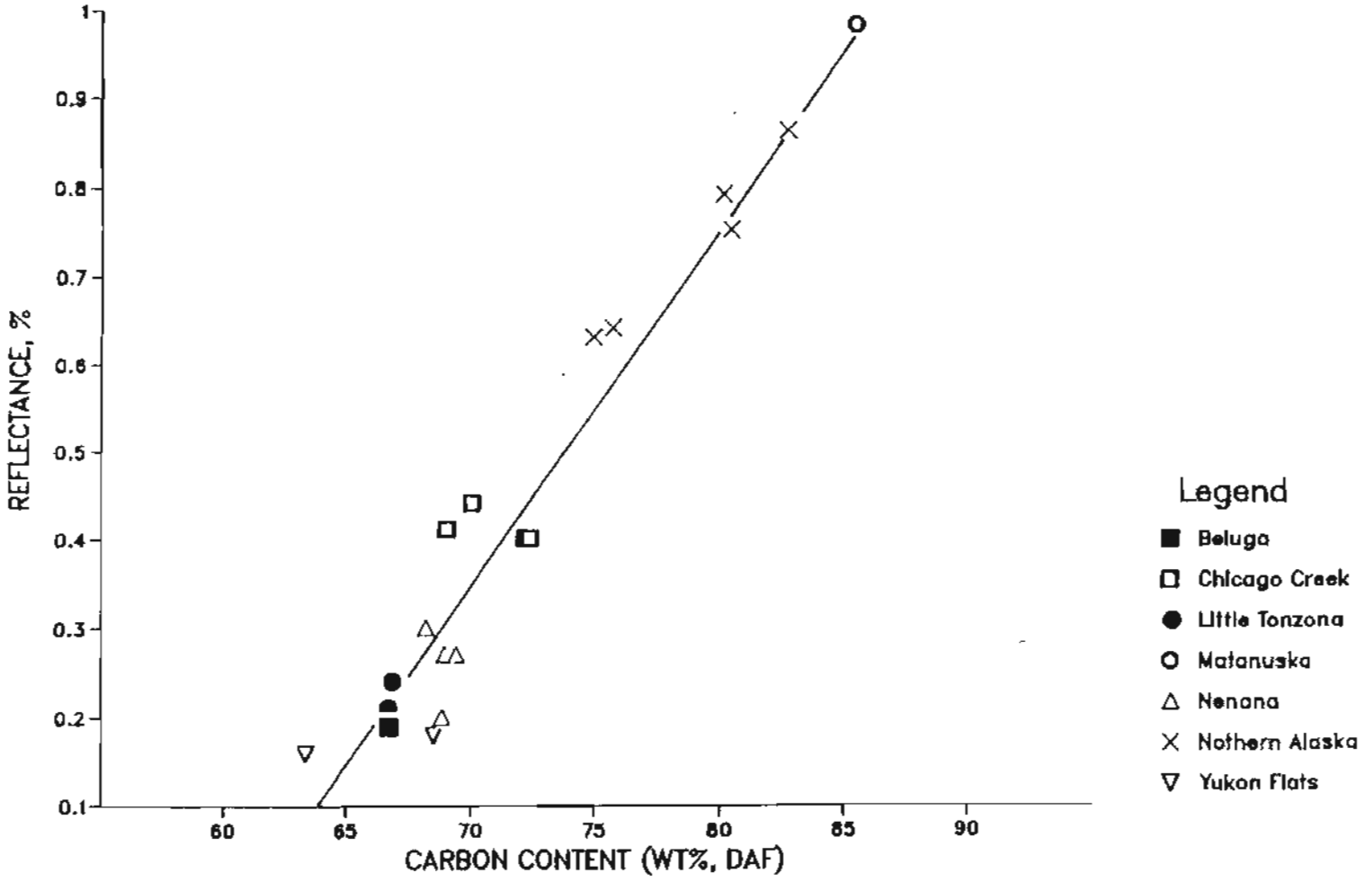

Figure 4. Relationship of $\bar{R}_{omax}$ with carbon content.

Table 3

Forms of Oxygen in Coals in Sample Set[a]

Sample ID	Total O	O as COOH	O as COO^-	O as OH	O unaccounted[b]
UA 148	26.03	3.78	0.83	7.22	14.20
DH 1-2	20.19	1.80	2.1	6.21	10.08
DH 1-4	20.28	0.93	2.4	7.41	9.34
DH 1-5	21.74	1.36	1.9	7.36	11.12
DH 1-6	21.55	3.19	1.9	6.52	9.94
CS 41730	26.16	2.72	3.2	8.33	11.91
CS 41735	27.43	3.06	1.8	7.56	15.01
UA 107	6.07		0.32[c]	4.36	1.39
UA 119	24.93	1.42	3.8	6.66	13.05
UA 129	25.29	2.57	3.7	8.94	10.08
UA 130	24.41	0.66	3.6	5.66	14.49
2UCM -11	24.81	1.80	3.1	8.55	11.37
UA 139	18.25	1.52	2.0	8.85	5.88
SS 67-1	12.87		0.22[c]	4.10	8.55
SS 67-2	13.38		0.38[c]	3.72	9.28
SS 67-3	11.18	0.04	0.38	3.46	7.30
CSB 13	18.83	1.29	2.2	9.48	5.87
HZA	29.61	1.44	0.83	8.30	19.04
HZE	23.93		7.74[c]	6.69	9.50

a) As percentage of daf coal.

b) See text, difference between total oxygen and accounted oxygen.

c) Total carboxyls, includes both free and metal carboxylates.

This occurs when the acetate washing results in an exchange with cations associated with the clays or solublizes some of the mineral matter in the coal. For such cases the concentration of total carboxyl groups is listed. A column for unaccounted oxygen is also given. These values were calculated as the difference between total oxygen and the oxygen functional groups determined.

$$O_T - O_{COOH} - O_{COO-} - O_{OH} = O_{unaccounted}$$

This oxygen is most likely present in the coal structure as cyclic or linear ethers. It is also possible for this oxygen to be in the form of methoxy groups.

The total carboxyl and hydroxyl contents are plotted up as a function of carbon content in Figure 5. The trends shown here are similar to those reported in the literature (Blom, 1960). There is a decrease in both functional groups with increasing rank. This decrease becomes marked for coals with carbon contents in the range of 75-80%.

IV. CORRELATION OF LIQUEFACTION BEHAVIOR WITH COAL CHARACTERISTICS

The product distribution and conversion yields for 19 coals liquefied for 3 and 30 minutes, are tabulated in Tables 4 and 5, respectively. Total conversion is defined as the sum of the yields of hexane solubles + gases, asphaltenes, and preasphaltenes. The values shown are the average of duplicate runs. Runs with short contact times were conducted to identify differences in reactivities of the individual coals. However, the conversion of a coal at 30 minutes, was found to mirror that of the short contact run.

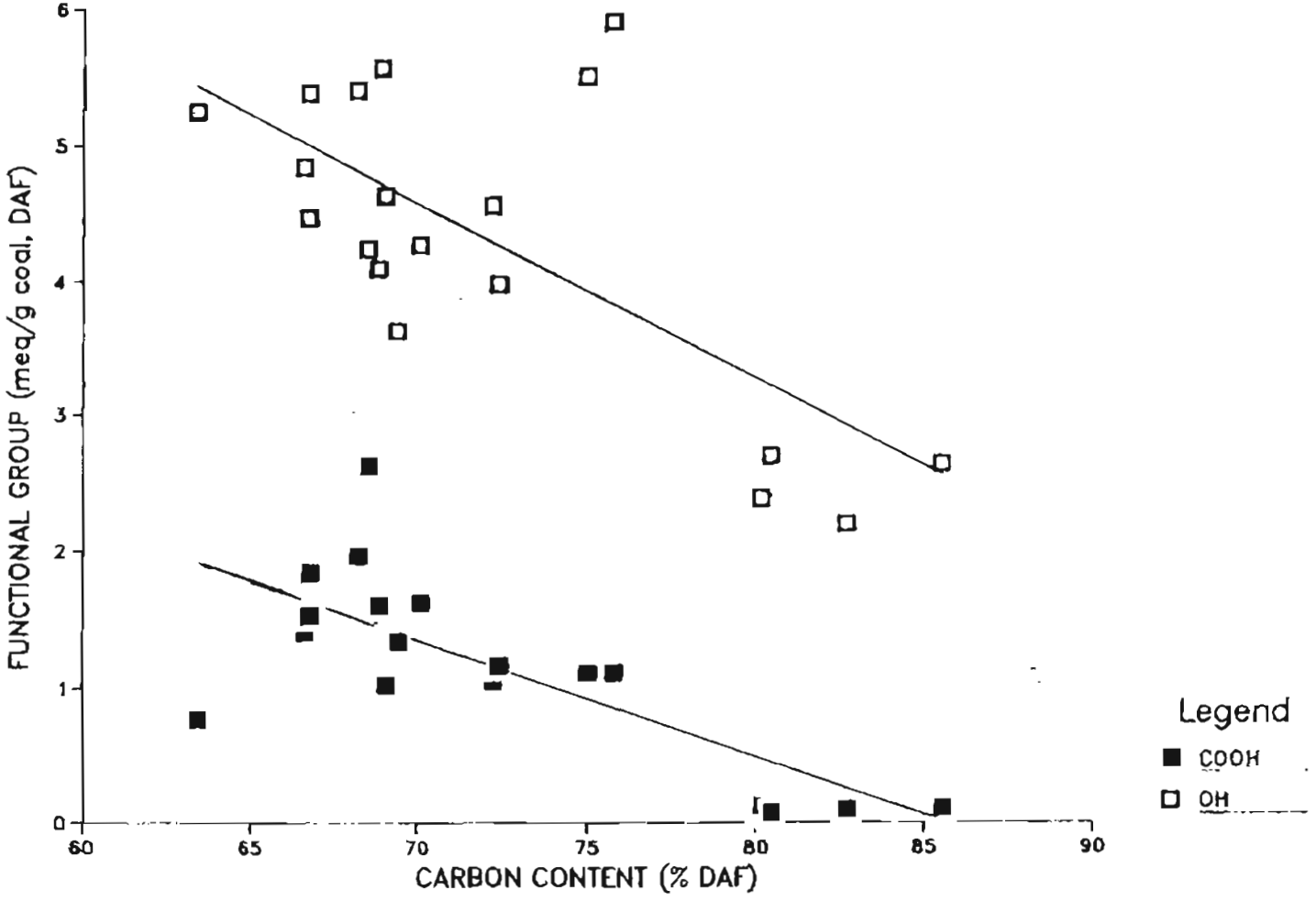

Figure 5. Relationships between oxygen functional groups and carbon content.

Table 4

Product Distribution

Reaction at 425°C, 3 minutes

COAL FIELD	SAMPLE NUMBER	Yields* ASPHALTENES	PREASPHALTENES	TOTAL** CONVERSION
Beluga	UA-148	12.34	13.22	64.82
Chicago Creek	DH 1-2	6.23	8.99	45.03
	DH 1-4	17.23	8.43	56.47
	DH 1-5	19.94	9.95	60.68
	DH 1-6	11.99	6.74	46.36
Little Tonzona	CS-41730	12.89	9.69	68.62
	CS-41735	10.94	9.96	72.53
Matanuska	UA-107	11.75	20.58	42.20
Nenana	UA-119	11.92	6.54	58.45
	UA-129	10.81	8.14	60.05
	UA-130	8.92	12.43	63.65
	2UCM-11	13.51	9.39	61.49
Northern Alaska	UA-139	5.33	11.74	40.49
	SS-67-1	19.52	23.10	59.33
	SS-67-2	21.59	7.34	41.26
	SS-67-3	15.79	9.47	32.95
	CSB-13	6.81	7.53	30.73
Yukon Flats	HZA	8.22	13.06	75.48
	HZE1	15.80	6.64	63.45

* Expressed on a wt%, daf basis

** Σ(oil + gases) + asphaltenes + preasphaltenes

Table 5

Product Distribution

Reaction at 425°C, 30 minutes

COAL FIELD	SAMPLE NUMBER	Yields* ASPHALTENES	PREASPHALTENES	TOTAL** CONVERSION
Beluga	UA-148	11.98	13.28	86.33
Chicago Creek	DH 1-2	10.97	12.14	74.27
	DH 1-4	18.05	13.69	85.48
	DH 1-5	16.12	8.19	82.35
	DH 1-6	15.94	5.68	72.70
Little Tonzona	CS-41730	10.12	11.43	88.87
	CS-41735	13.13	8.81	86.32
Matanuska	UA-107	32.48	16.58	68.88
Nenana	UA-119	9.86	12.06	86.36
	UA-129	12.19	5.91	84.60
	UA-130	13.02	11.86	88.67
	2UCM-11	13.32	12.04	87.37
Northern Alaska	UA-139	15.63	10.83	60.61
	SS-67-1	29.40	19.56	77.65
	SS-67-2	23.16	15.95	65.07
	SS-67-3	20.72	13.54	55.85
	CSB-13	16.41	13.22	60.73
Yukon Flats	HZA	16.73	6.68	91.65
	HZE1	23.76	9.68	76.72

* Expressed on a wt%, daf basis

** Σ(oil + gases) + asphaltenes + preasphaltenes

The low rank coals from the Nenana, Little Tonzona and Beluga coal fields give rise to products that are highly soluble in THF, whereas, the coals from the Matanuska, Northern Alaska and Chicago Creek coal fields are considerably less reactive, and the coals from the Yukon Flats are of variable reactivity. Differences in reactivities become apparent when the product slates are compared.

In general, high concentrations of higher molecular weight products, namely, asphaltenes and preasphaltenes coincide with coals with high inertinite contents. However, samples UA-107 and SS-67-1 gave rise to the highest concentration of preasphaltenes in both the 3 and 30 minute runs, and both of these are low inertinite, high rank coals. An unusual feature of these coals is their high pseudovitrinite content. This appears to be readily converted, though most of it ends up as preasphaltenes. With time this product is converted into smaller units such as asphaltenes or oil.

In order to evaluate how various coal characteristics influence the conversion yield of Alaskan coals, bivariant plots were constructed. In Figure 6 is illustrated the relationships between carbon content and conversion of coal to THF solubles plus gases. The trend for conversion yields to increase with decreasing carbon content are quite similar for both the 3 minute and 30 minute runs.

Carbon content is not a good correlation parameter since it fails to take into consideration the fact that several of the coals may have undergone some weathering prior to their sampling. The Cape Beaufort coals (UA-139 and CSB 13) from Northern Alaska are not deeply buried and may have been oxidized due to their close proximity to the

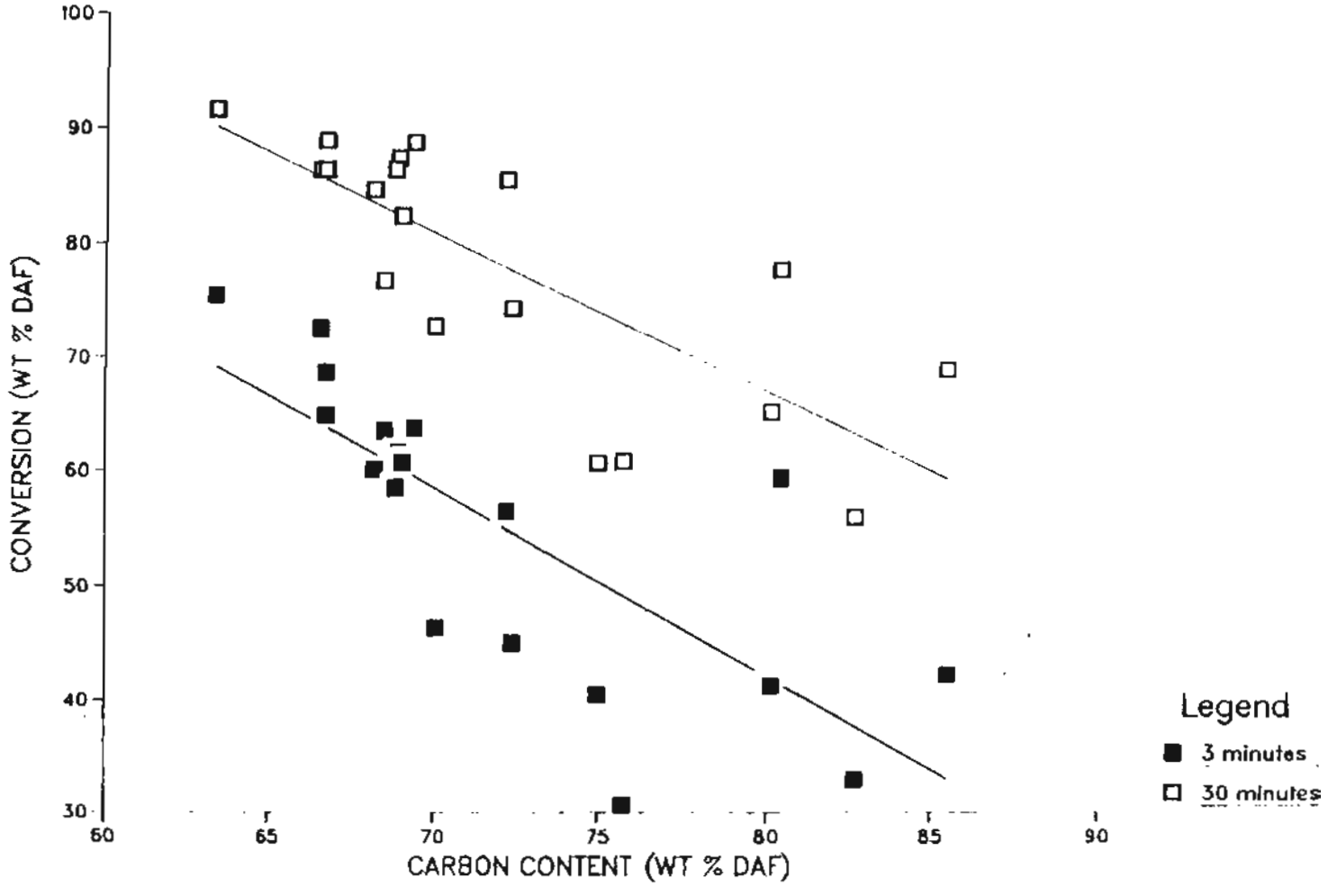

Figure 6. Correlation of conversion with carbon content.

surface. The Matanuska coal (UA-107) is another sample which is suspect in this regard, as it was taken from an old mine exposure.

The correlation between volatile matter, a rank parameter, and conversion yield is shown in Figure 7. A linear least squares analysis of this data gives an R^2 factor of 0.759. Data for both the inertinite rich high rank Northern Alaska and the low rank Chicago Creek coals show a considerable amount of scatter in this plot, whereas the data for the reactive coals taken from the same coal field, tend to cluster.

These rank trends are not in agreement with the findings of Given and others (1975a) and Whitehurst and co-workers (1979). Their investigations of the influence of rank parameters indicated that subbituminous coals were significantly more difficult to liquefy than bituminous coals and that maximum conversion occurs for coals of high volatile bituminous rank. The source of this difference in trends appears to be the nature of the solvent used in the various studies. Experiments conducted here involved using a large excess of tetralin. In the other two studies, a process solvent was used. The demand for hydrogen is considerably greater when liquefying low rank coals. Presumably, the excess tetralin is able to accommodate this demand whereas the process solvent is not.

The effect of reactive macerals (vitrinite + exinites) on short contact time conversion was examined. This is plotted in Figure 8. This dependence should be more pronounced than that with longer contact time yields since the liptinites are generally considerably more reactive than the inertinites. What is found is that two

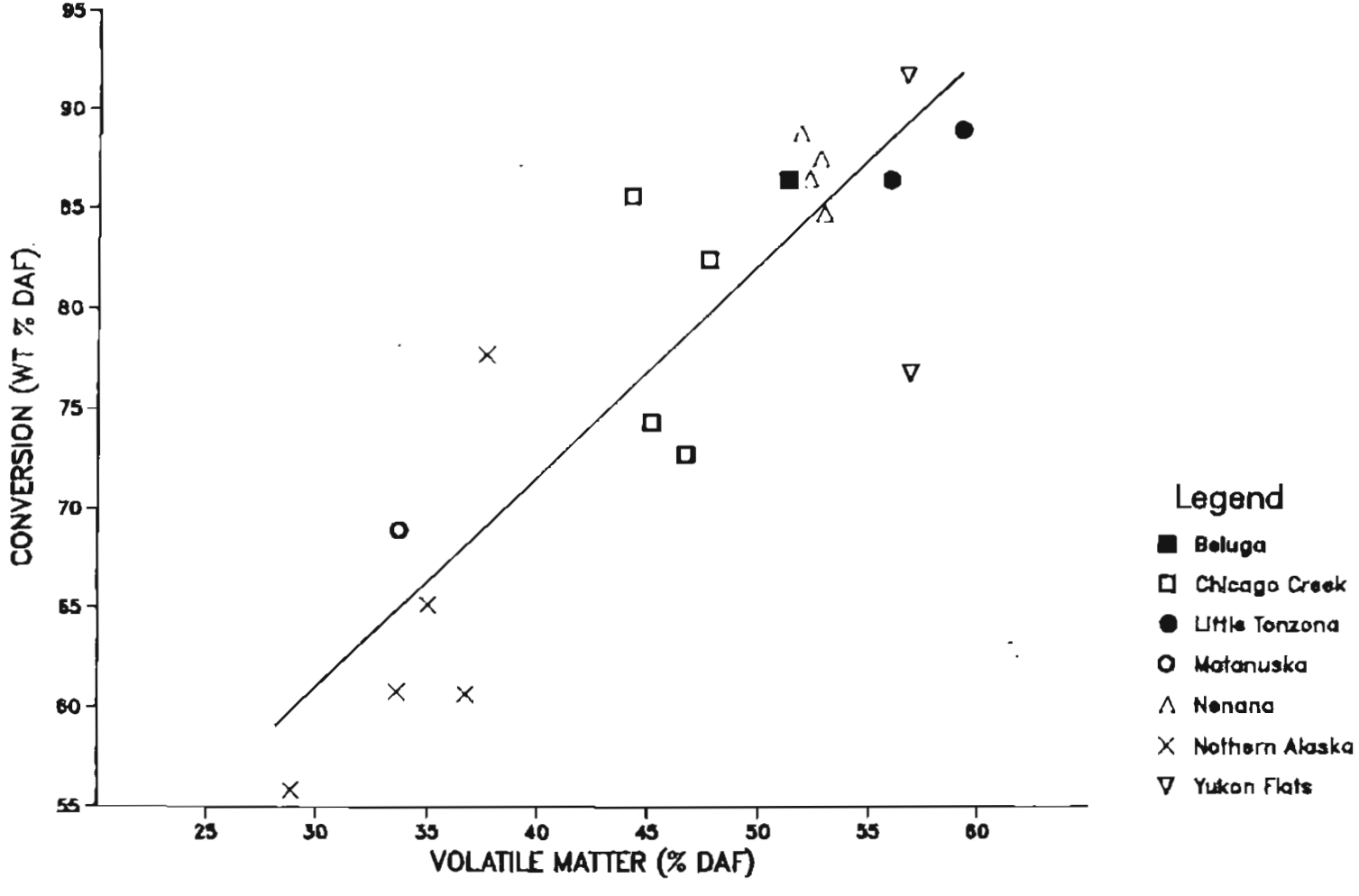

Figure 7. Dependence of conversion on volatile matter content.

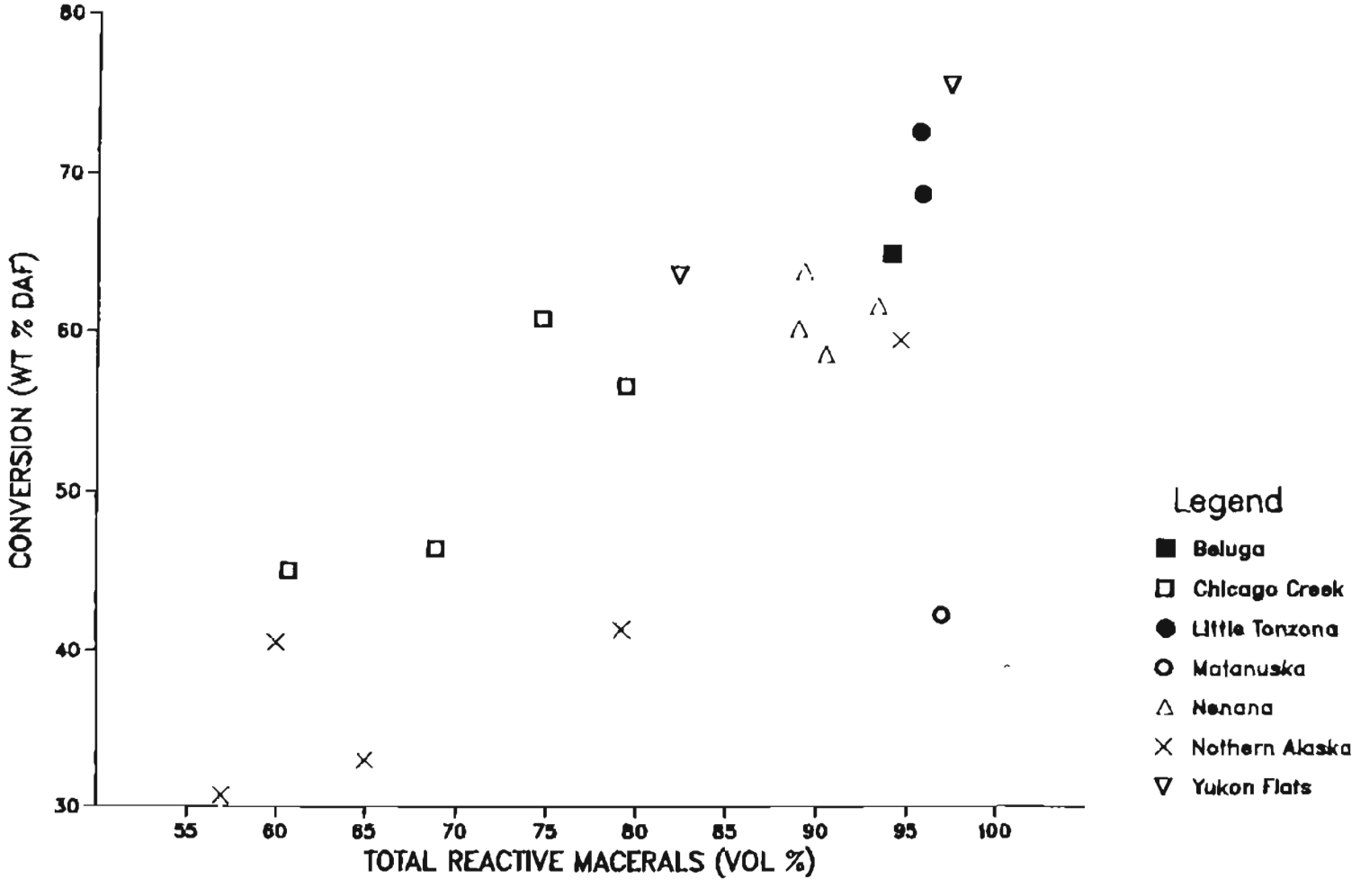

Figure 8. Dependence of conversion on content of reactive macerals.

relationships between conversion and total reactive macerals exist. A strong dependence is exhibited by the low rank Tertiary coals and little if any correlation is shown for the bituminous Cretaceous coals.

The Nenana coals contain an abundance of exinites and gave very high conversion yields, while the Northern Alaskan coals, particularly the Cape Beaufort coals (UA-139 and CSB-13), which consist of 40% inert macerals, were the least readily converted. The reason for the Matanuska coal's low conversion yield is not apparent, particularly since this coal contains the least amount of inertinite macerals.

The oil and gas yield was found to make up a considerable percentage of the overall conversion product. This product fraction expressed as a percentage of the total yield also correlates surprisingly well with carbon content (R^2 of .926). This correlation is plotted in Figure 9. Even though the oil plus gas yields are obtained by difference, associated errors should be consistent for all runs and should not be biased by rank. One would anticipate the total gas product to increase with decreasing rank of coal, however this alone fails to explain the success of this correlation.

Recently, Given and Derbyshire (1985) found higher oil to asphaltene ratios in catalytic hydrogenation products of lower rank coals. Their interpretation of this behavior is that low rank coals are bridged by labile species which are readily cleaved under liquefaction conditions. However, thermal hydrogenation reactions often are not able to compete with condensation reactions, and this would give rise to higher asphaltene and preasphaltene concentrations

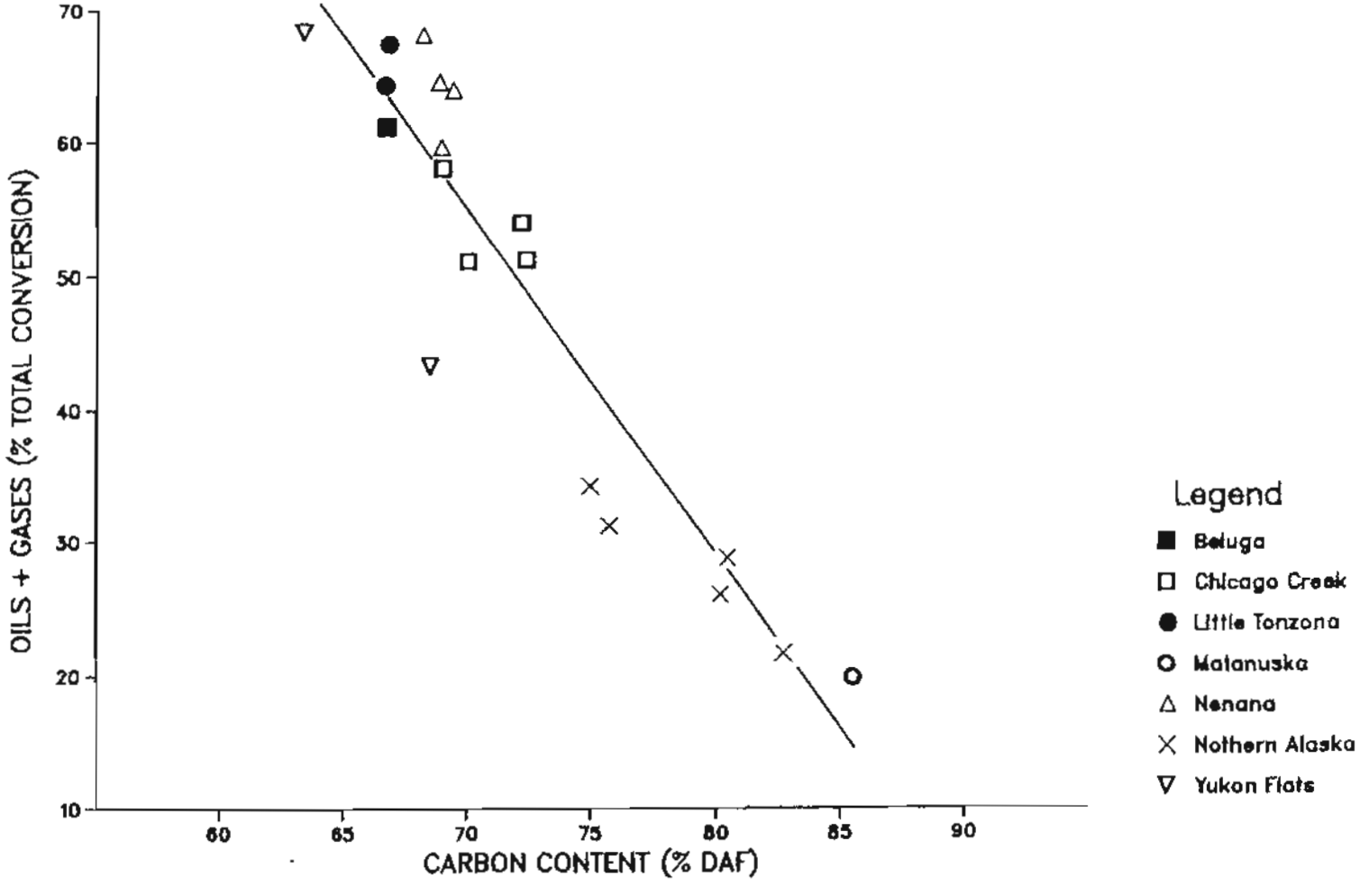

Figure 9. Correlation of the oil and gas fraction of converted products with carbon content.

in the products and may even result in reduced conversion yields. In the higher rank coals, diffusion limitations seem to be enhancing the condensation reactions relative to hydrogen capping.

Liptinites are often considered to be both highly aliphatic and very reactive. Consequently one would expect to see an influence on the oil + gas product fraction by these hydrogen rich macerals. This fraction is plotted against reactive maceral content in Figure 10. The trend follows that of Figure 8. This suggests that the vitrinite in the low rank coals is as important, if not more so than the liptinite, in determining oil + gas yield.

Though such bivariant plots are overly simplistic, as pointed out by Given and others (1982), they are valuable for indicating rough trends for coals of different provinance. Overall these trends are in agreement with those in the literature (see for example Yarzab et al., 1980; Given et al., 1982).

The importance of ether cleavage in coal liquefaction behavior was examined by Youtcheff (1983). In this study the maximum number of cleavable ethers was found to be both rank-dependent and geologic-province-dependent. In light of this, the dependence of conversion at short contact time with unaccounted oxygen was examined. This is plotted in Figure 11. The early stages of coal liquefaction are characterized by limited bond cleavage and limited hydrogen transfer from the solvent. Consequently, if the unaccounted oxygen is present as labile ether groups such as benzyl and aryl-alkyl ethers, a high degree of correlation is expected. A trend is evident in Figure 11 but there is a considerable amount of scatter. For example, the

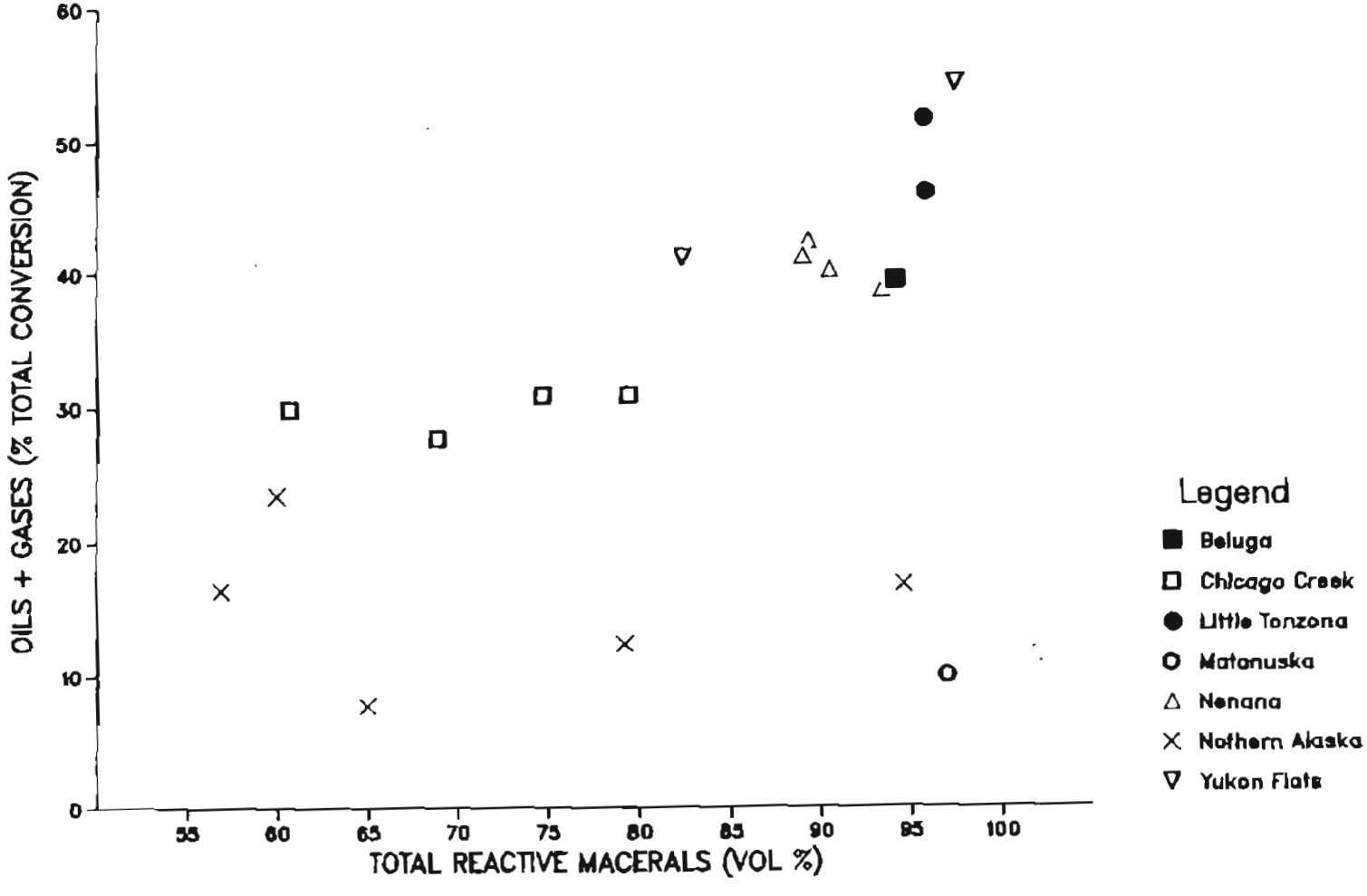

Figure 10. Relationship between the oil and gas fraction of converted products and reactive macerals.

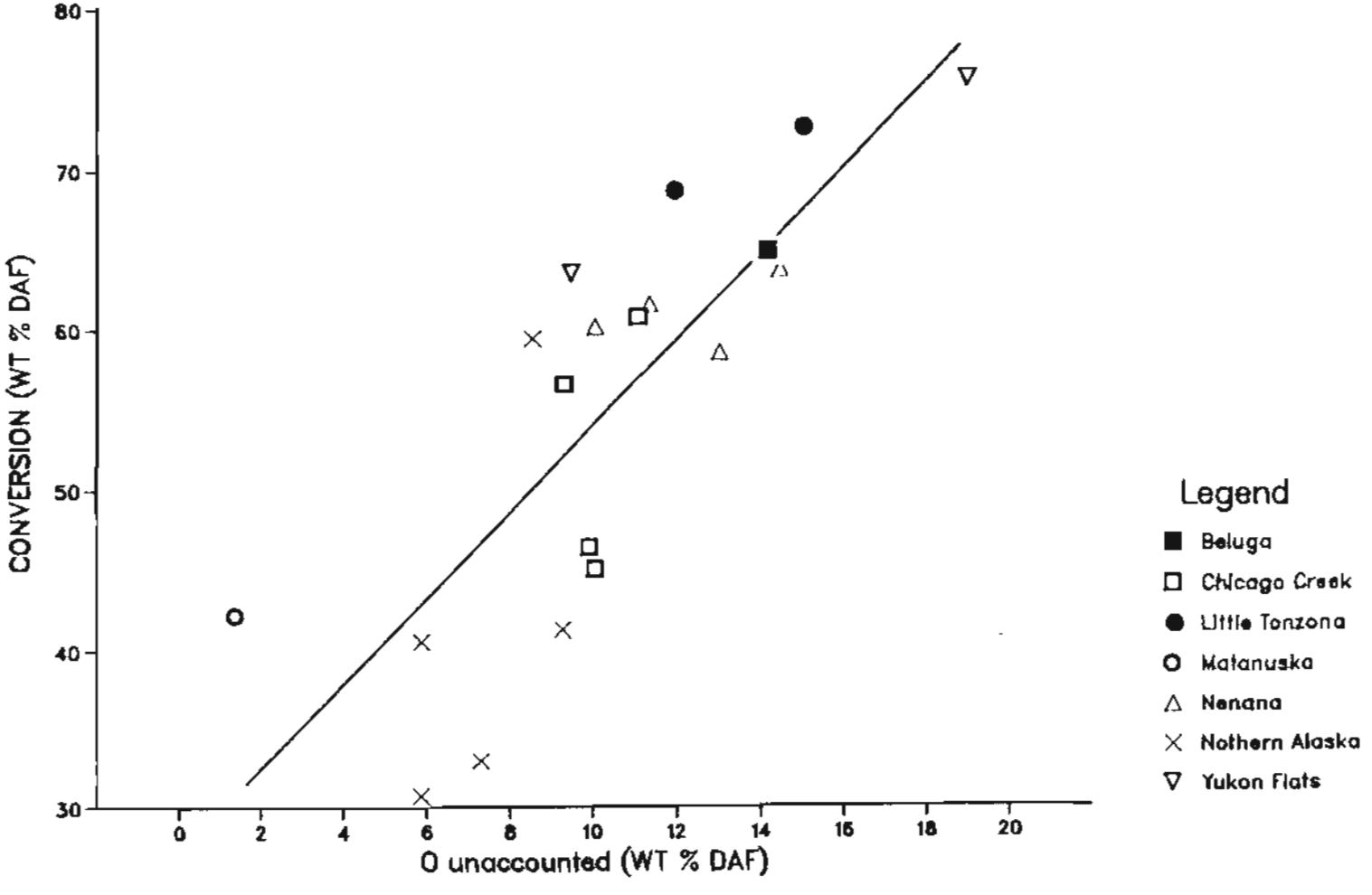

Figure 11. Dependence of conversion at short contact time with unaccounted oxygen.

unaccounted oxygen content is quite low in UA-107. Conversion of this coal most likely results from cleavage of methylene groups. In most of the inertinite rich coals, conversions fell below that expected from a least squares fit of the data. Presumably the unaccounted oxygen in these coals is present as stable aryl or cyclic ethers.

SPECTROSCOPIC EXAMINATION OF THE HEXANE-INSOLUBLES

Infrared spectra of the coals and hexane insoluble products were recorded. Our goal was to conduct preliminary investigations into the following areas:

(1) to identify possible evidence of long term coal oxidation resulting from natural conditions, particularly in samples CSB-13 and UA 139, and any evidence of short term oxidation on the surficial samples HZA and HZE1;

(2) to identify unusual structural features; special emphasis was placed on studying coals with unusual maceral distributions, such as the high concentration of fluorescent ulminite in the HZA sample and the high inertinite content associated with the Northern Alaska coals;

(3) to follow changes in spectral features as a function of liquefaction severity, and

(4) to identify changes associated with mineral matter.

Two coals were studied in detail, CSB-13, an inertinite rich coal and the unusual HZA coal. In Figure 12 is shown a DRIFT spectrum of CSB-13. The spectral features of this coal are quite similar to that found in the literature (see for example, Painter et al., 1985). The

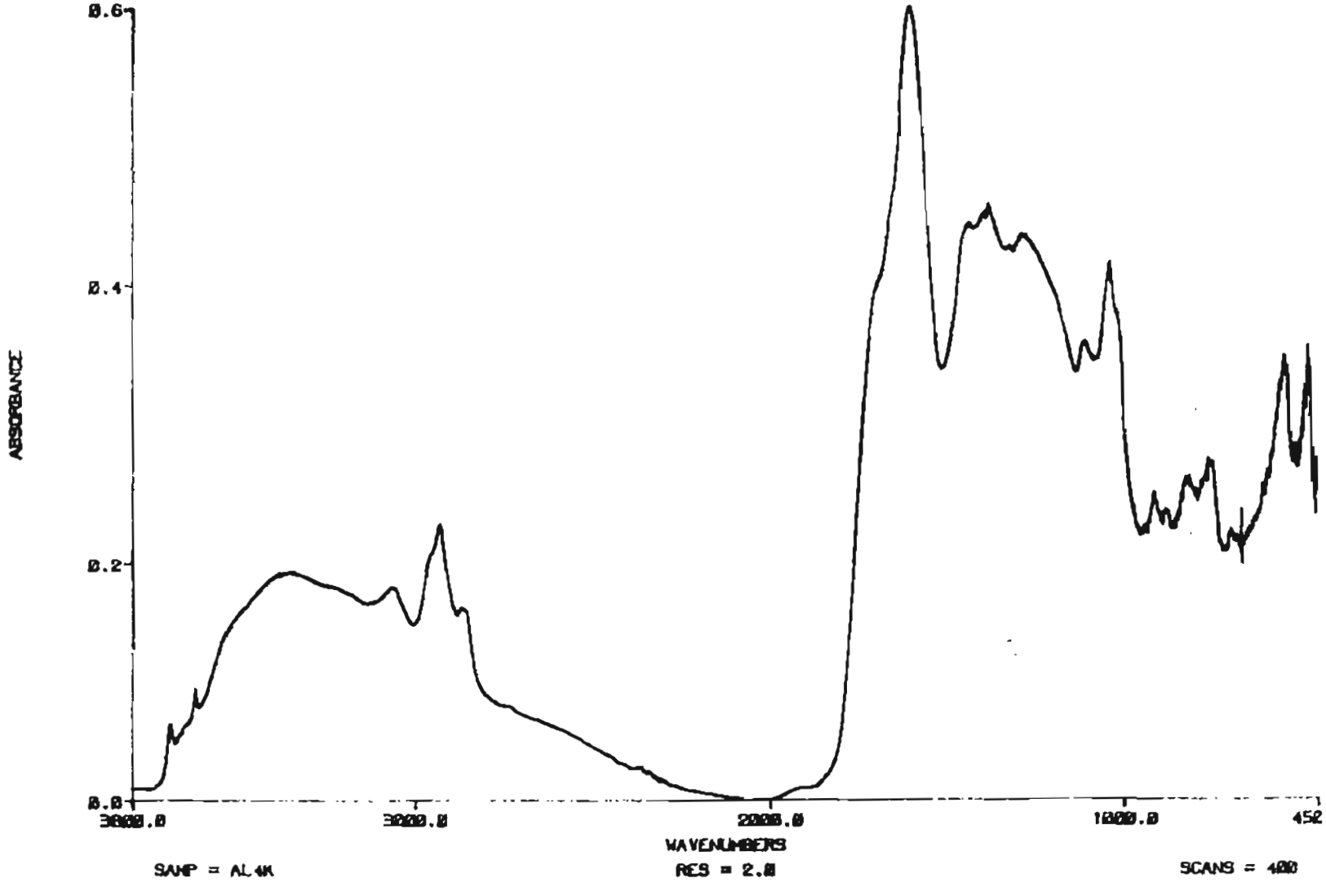

Figure 12. DRIFT spectrum of CSB-13.

spectrum of CSB-13 shows the presence of a slight shoulder at 1710 cm^{-1}; this is attributable to carboxyl groups. While such groups have been identified as products of oxidation (Painter et al., 1981), they are also found in low rank coals. In addition, if this coal had been oxidized and later subjected to circulating waters, ion exchange of the generated acid groups could conceivably take place. The band associated with the carboxyl group would then be shifted from the 1700 cm^{-1} region to around 1575 cm^{-1} and ultimately be masked by the C-C stretch band at 1600 cm^{-1}. Hence, this is hardly conclusive evidence for determining whether this particular coal has been oxidized or for determining the extent of the weathering.

An unusual feature of the CSB-13 spectrum is the exceptionally weak intensity of the aliphatic C-H bands in the 3000 - 2750 cm^{-1} region. In spectra of the other inertinite rich coals (SS 67-2, SS 67-3) examined, this is not observed; instead, rather intense aliphatic C-H bands are present. These observations give credence to attributing the weak aliphatic C-H signal in the CSB-13 spectrum due to effects of oxidative weathering. One consequence of this is that relatively few cleavable aliphatic linkages may be present in this coal. In addition, the unaccounted oxygen content of this coal is quite low (5.87%) relative to the other coals in the sample set. Presumably this coal is deficient in labile linkages such as benzyl ethers, dibenzyl, etc. This is one plausible explanation for the low conversion yields obtained from this coal. Examination of the spectrum of the HI product (Figure 13) seems to agree with this hypothesis. The intensity of the aliphatic C-H region is still quite

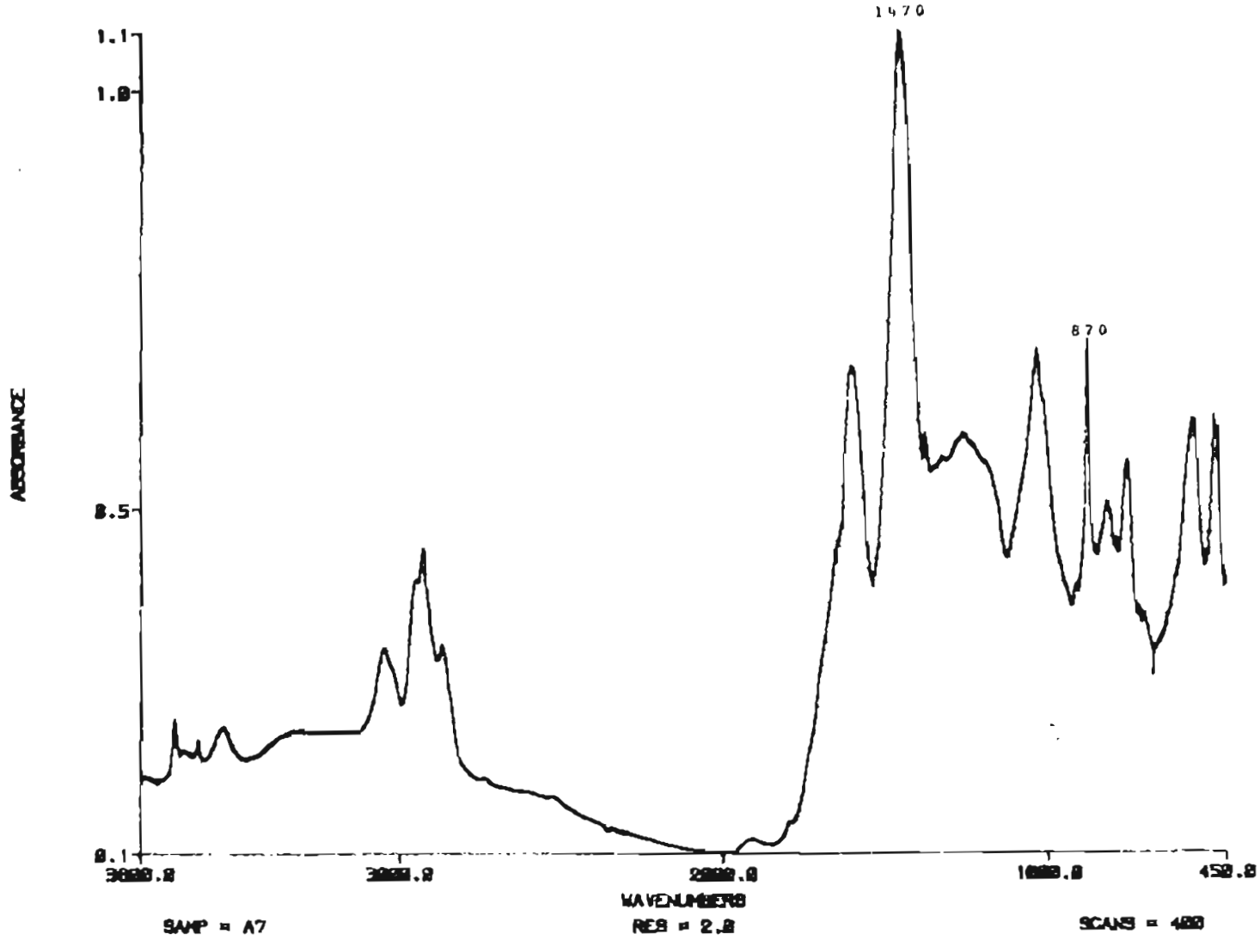

Figure 13. DRIFT spectrum of hexane insolubles from CSB-13. (Coal liquefied at 425^{0}C/0.5 hr)

weak although it has increased relative to the 1600 cm^{-1} band. The changes in the aliphatic C-H region are apparent in Figure 14. These spectra show a systematic increase in the intensity of aromatic C-H absorption at 3050 cm^{-1} and changes in aliphatic C-H bands as a function of liquefaction severity. The latter are attributable to an increase in methyl groups. Qualitatively, the changes seen here were the least dramatic of all the coals examined.

There are some additional peaks which are present in the HI spectrum (Figure 12) that are not in the spectrum of the parent coal (Figure 11). The absorption bands at 1470 and 870 cm^{-1} are vibrations associated with vaterite, a calcium carbonate. These bands were found in almost all of the spectra of HI generated at 32 minutes. No evidence of vaterite formation was seen in the HI products from SS 67-2 and SS 67-3. Presumably, with such low carboxyl contents (see Table 3) the formation of vaterite is negligible.

The spectral features of HZA are quite unique for a coal. An FTIR spectrum of this coal is shown in Figure 15. It is interesting to note that many of these features are similar to those found in lignin. Rhoads (1985) separated lignin from a number of peats. Spectra of several of these lignin are shown in Figure 16. The spectrum of the Taxodium (Cypress) lignin is especially similar to that of HZA. Features such as the bands attributed to aromatic skeletal vibrations at 1510 and 1420 cm^{-1}, the bands at 1140 and 1030 cm^{-1} assigned to ArCH in plane deformations, and peaks at 1256 and 1220 cm^{-1} assigned to ring breathing modes with C-O stretch are common to both spectra. The relative intensity of many of these bands have

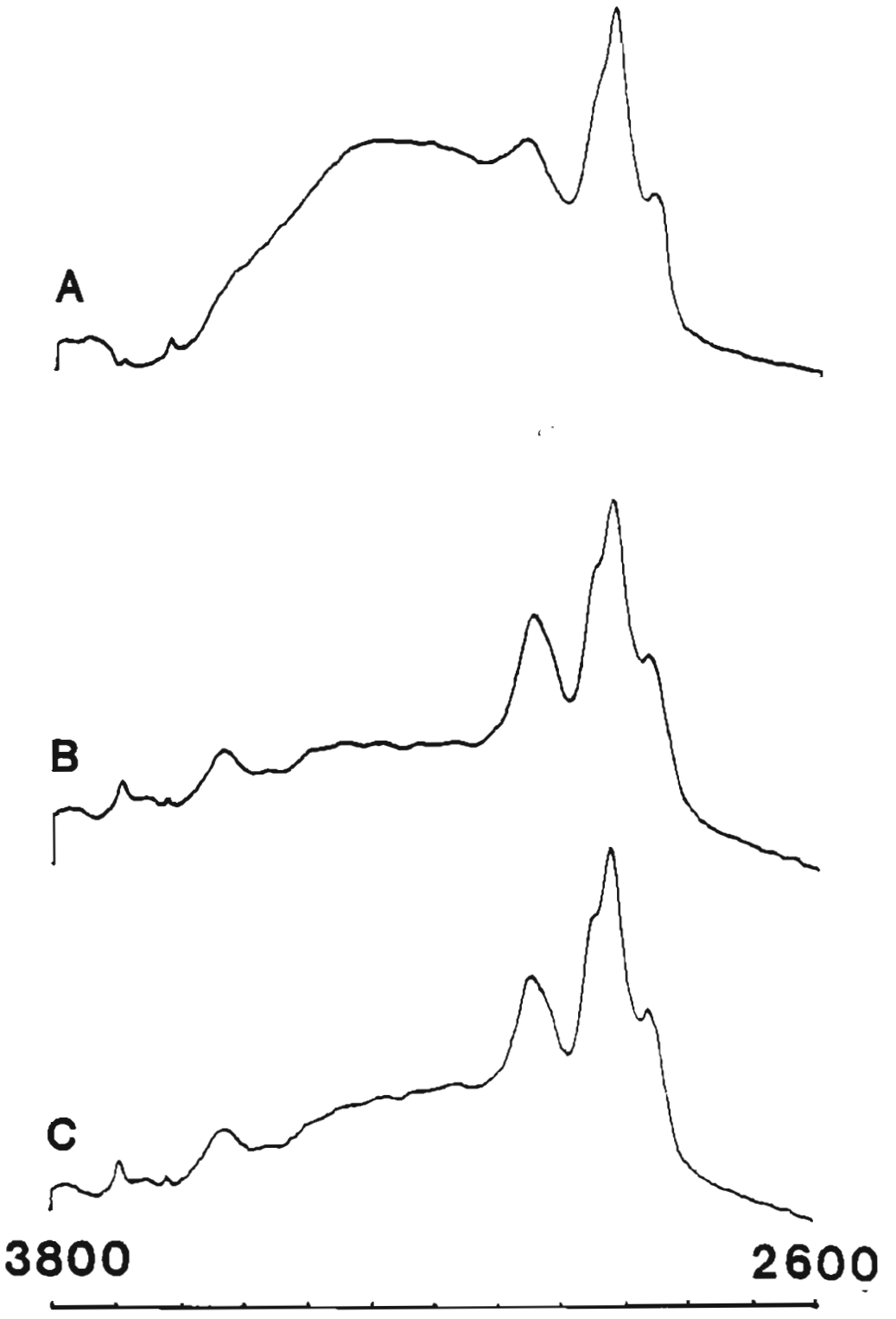

Figure 14. DRIFT spectra of hexane insolubles from liquefaction of CSB-13.

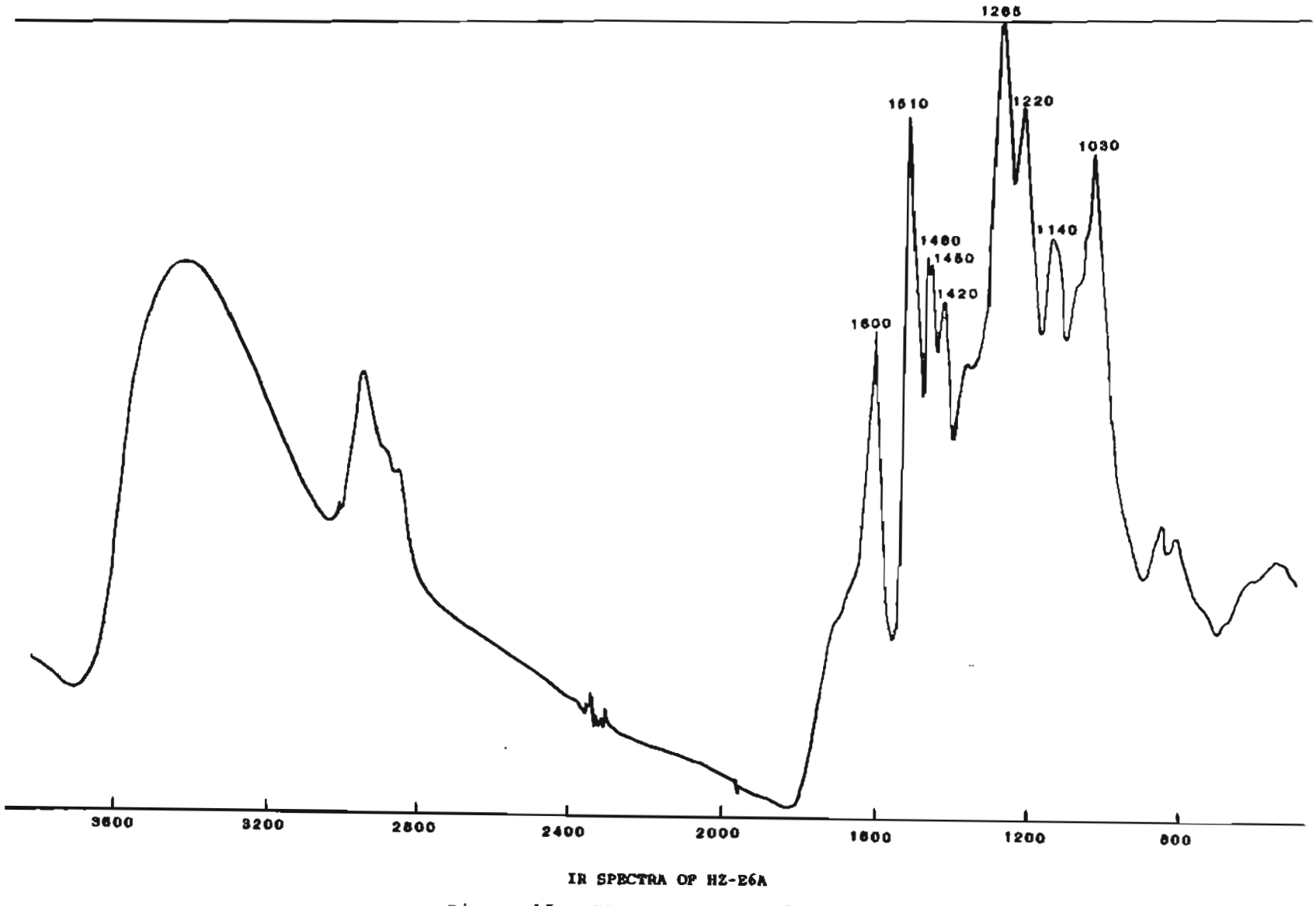

Figure 15. FTIR spectrum of HZA

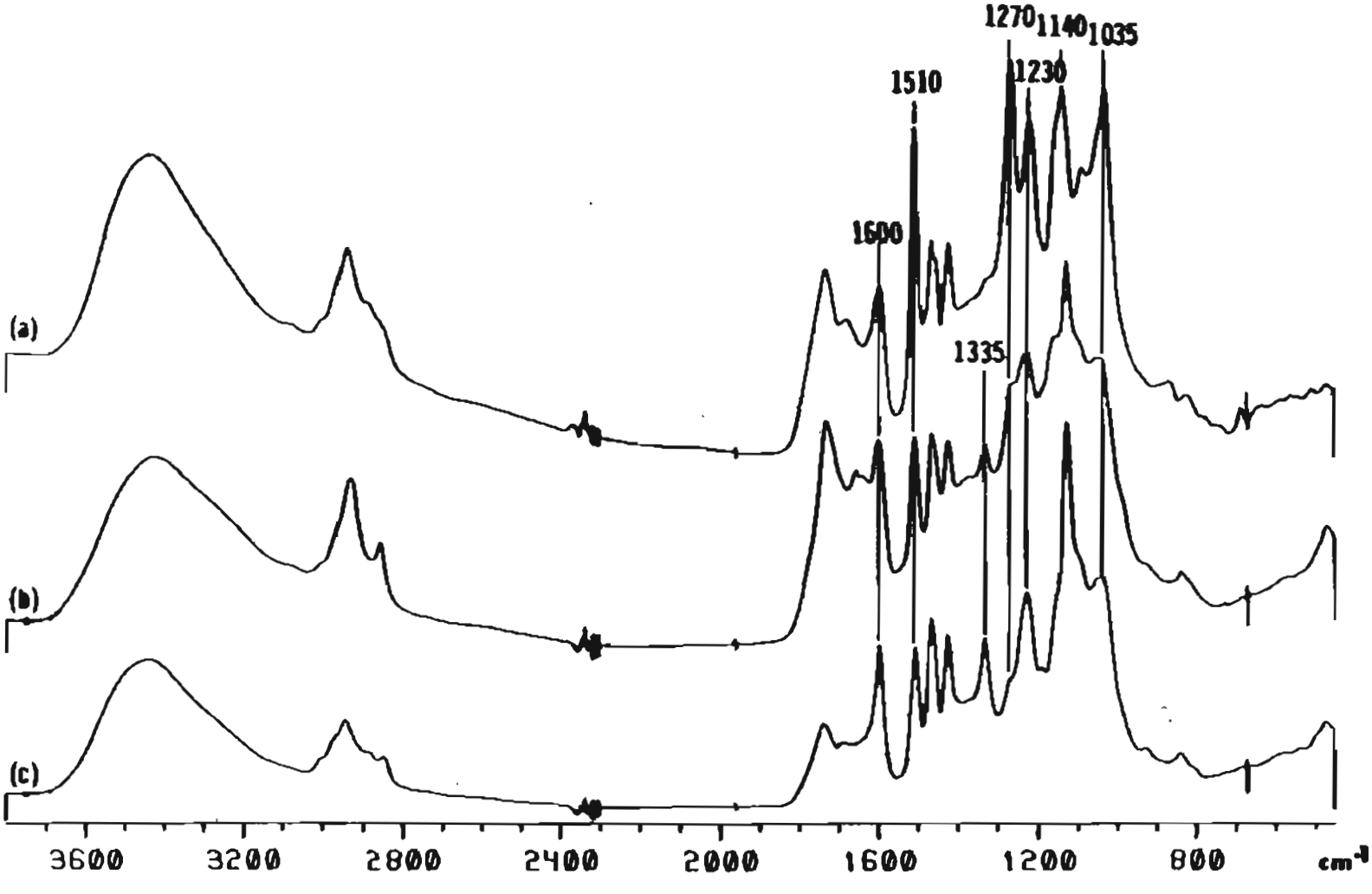

Figure 16. **SPECTRA OF PERIODATE LIGNINS**
Spectra of: (a) Taxodium (b) Juncus (c) Rhizophora
(from Rhoads, 1985)

been used to distinguish the lignin-type. Hergert (1971) reported that a softwood or guaiacyl type lignin is suggested when the 1270 cm^{-1} band is more intense than the 1230 cm^{-1} band and the 1035 cm^{-1} band is greater or equal to the intensity of the 1140 cm^{-1} band. This type of lignin, which is found to occur in conifers and pre-gymnosperms, is principally a homopolymer of coniferyl alcohol (Given, 1984). Additional evidence for comparison of the two spectra is the presence of a weak methoxyl absorbance at 3000 cm^{-1}.

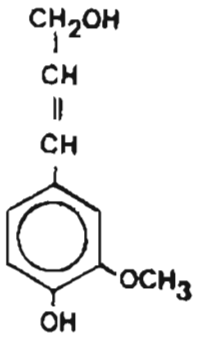

Coniferyl Alcohol

The effect of liquefying this coal for varying durations was investigated. DRIFT spectra of the raw coal and hexane-insolubles product (HI) are shown in Figure 17. By the time this coal is heated to the reaction temperature, most or all of the groups which give rise to absorptions at 1140 and 1035 cm^{-1} are lost or converted. Presumably these structures are methoxyl groups, but the contribution of aliphatic ethers and alcohol groups cannot be ruled out. The intensity of the aromatic skeletal vibrations are also considerably reduced. It is unlikely that these groups are condensing together and forming larger aromatic moeities but rather that they are converted into a hexane soluble product and are selectively reduced in abundance. Other changes evident in this spectrum include the development of C-H out-of-plane bending modes (900-700 cm^{-1}) and a

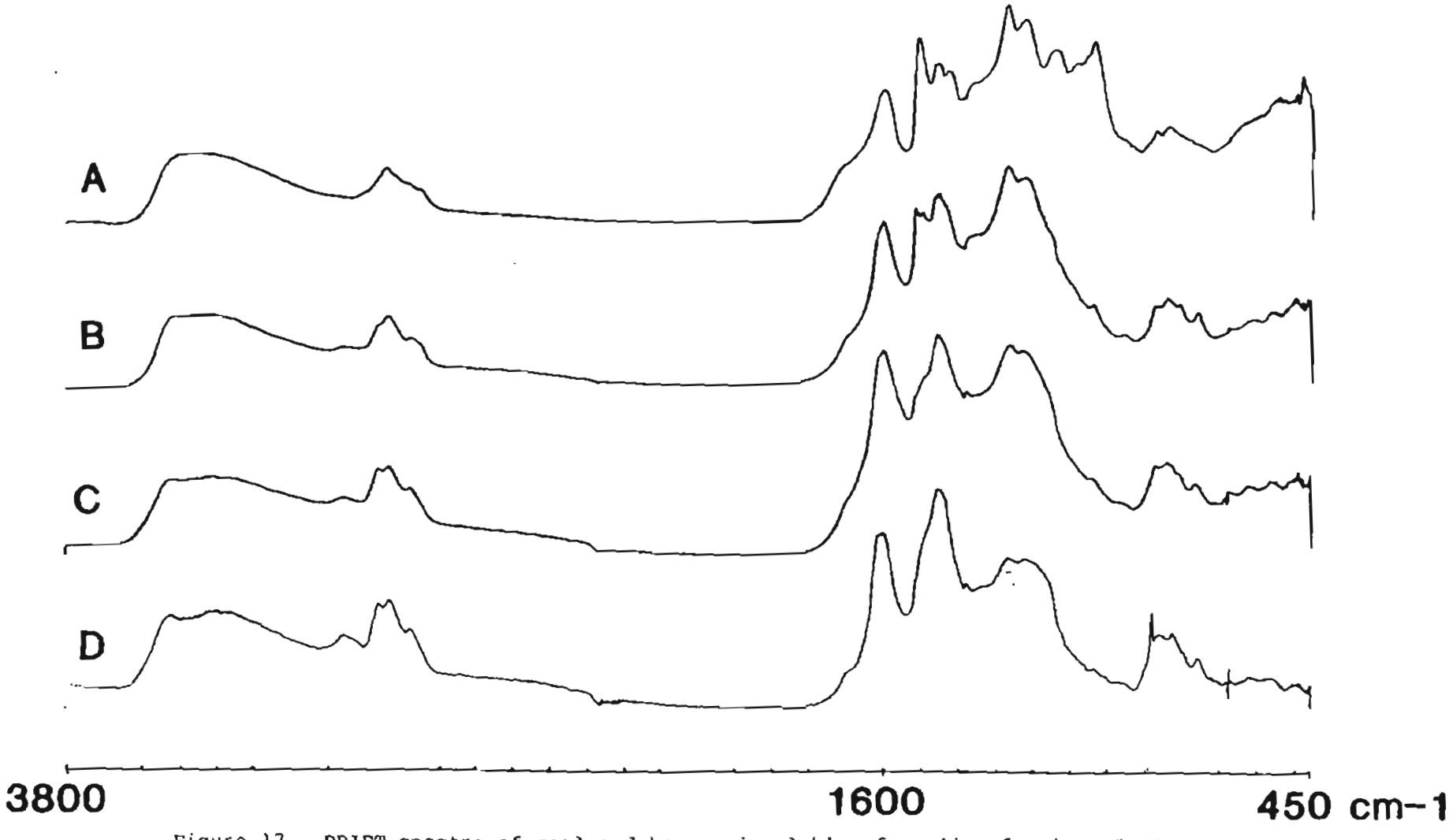

Figure 17. DRIFT spectra of coal and hexane insolubles from liquefaction of H2A. (a) Original coal; (b) 0 min at 425°C; (c) 3 min at 425°C; (d) 30 min at 425°C.

reduction in the carboxyl region (shoulder at 1700 cm^{-1}).

The spectrum of the HI product formed in a three minute run takes on the appearance of spectra typical for coal (Painter et al., 1985). All semblances of the aromatic skeletal vibrations are lost. These peaks blend together into a single band at 1450 cm^{-1} which is assignable to CH_2 and CH_3 bending modes. After 30 minutes residence time the 1450 cm^{-1} band shifts to 1470 cm^{-1} and a sharp peak at 870 cm^{-1} is present. Both of these changes are associated with vaterite formation. In addition the 1330 - 1110 cm^{-1} region (attributed to CO stretch and OH bend in phenoxy structures and ethers) is considerably reduced.

The intensity of the aliphatic C-H stretch region appears to remain constant. However, there are a number of changes apparent in the spectra of this region, as shown in Figure 18, that are occurring during the course of liquefaction. Methoxyl groups (3000 cm^{-1}) are readily lost, and there is an increase in the intensity of aromatic C-H groups (3050 cm^{-1}) and aliphatic CH_3 (2956 cm^{-1}) as a function of time. These changes are much more striking when spectral subtraction is applied. In Figure 19, spectra of HI from a 30 minute run, a 3 minute run and their difference are shown.

BEHAVIOR OF SELECT MACERALS UNDER LIQUEFACTION CONDITIONS

One of our objectives was to conduct a preliminary evaluation regarding the nature and behavior of fluorescent vitrinites and inertinite macerals. Several of the coals in the sample set are well suited to such a study.

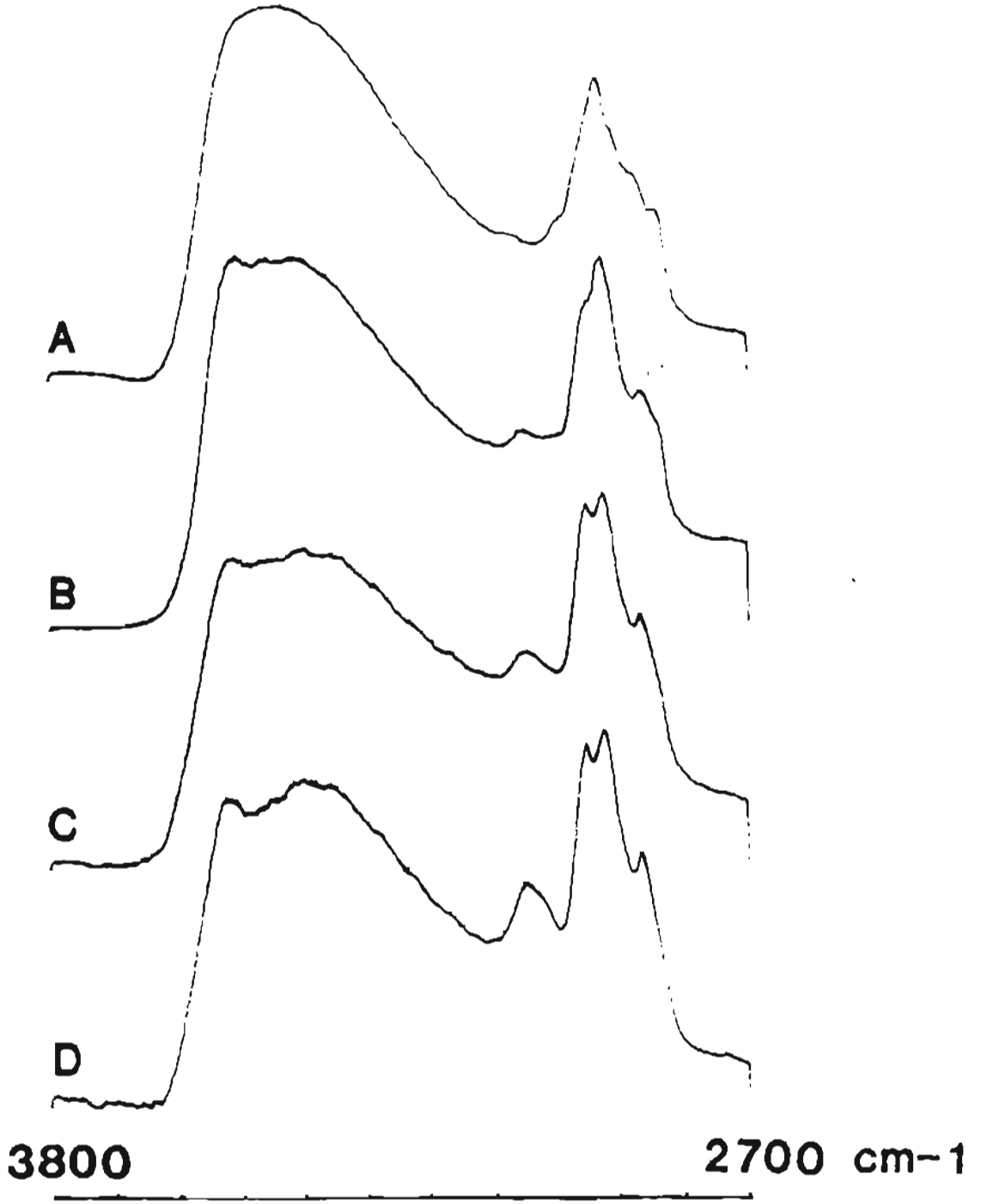

Figure 18. Partial DRIFT spectra of coal and HI from liquefaction of HZA. (a) raw coal; (b) 0 min at 425°C; (c) 3 min at 425°C; (d) 30 min at 425°C.

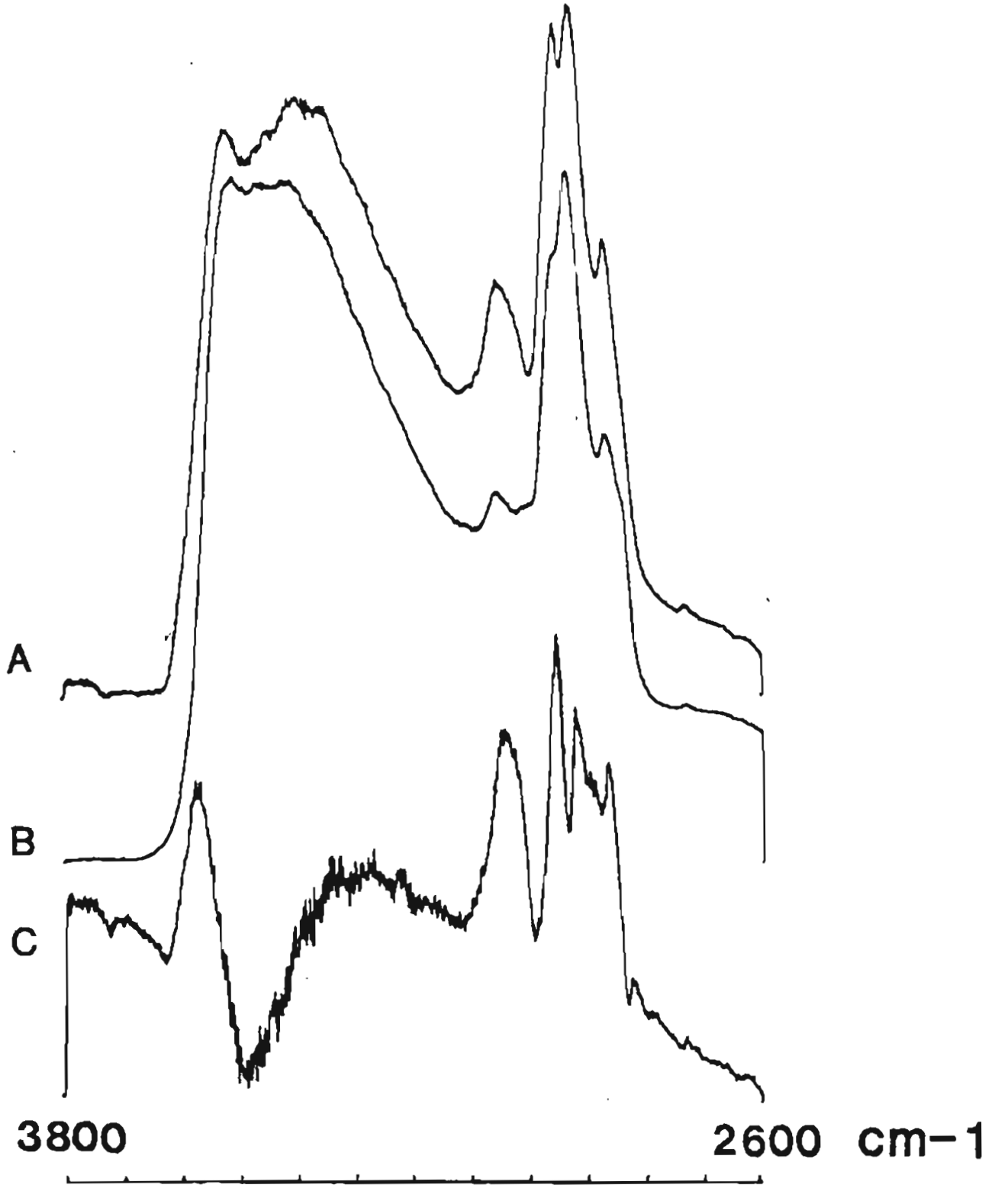

Figure 19. Spectral subtraction of H2A liquefaction product.
(For hexane insolubles generated at 425°C)
(a) 30 min run; (b) 0 min run; (c) difference spectrum.

a) Fluorescent Vitrinites

Our particular interest in this maceral was in ascertaining if these perhydrous vitrinites are rich in donatable hydrogen. If so, excellent conversions could be expected for such coals. The internal hydrogen donors would not only be able to help satisfy the demand for hydrogen but would also be able to cap radicals generated in close proximity. The importance, with regards to the latter, is that the propensity for retrogressive reactions during the early stages of liquefaction would be greatly reduced.

Two of the coals in the sample set were found to have high fluorescent ulminite contents. One is from the Little Tonzona coal field (CS 417-30), and the other is from the Yukon Flats (HZA). These lithotypes account for 19.4 and 76.8 (Vol %, mmf) of these coals, respectively. Due to time constraints, structural characterization of the HZA sample was limited to spectral interpretation of DRIFT spectra. Though no studies were conducted to correlate structural features with fluorescence spectra, the results of some preliminary studies are reported.

In generating a fluorescence spectrum, HZA was subjected to an irradiation period of 30 minutes. Spectral scan measurements were taken at 1, 5, 10, 20 and 30 minutes. Progress of the alteration are shown in Figure 20 and characteristics of these spectra are listed in Table 6.

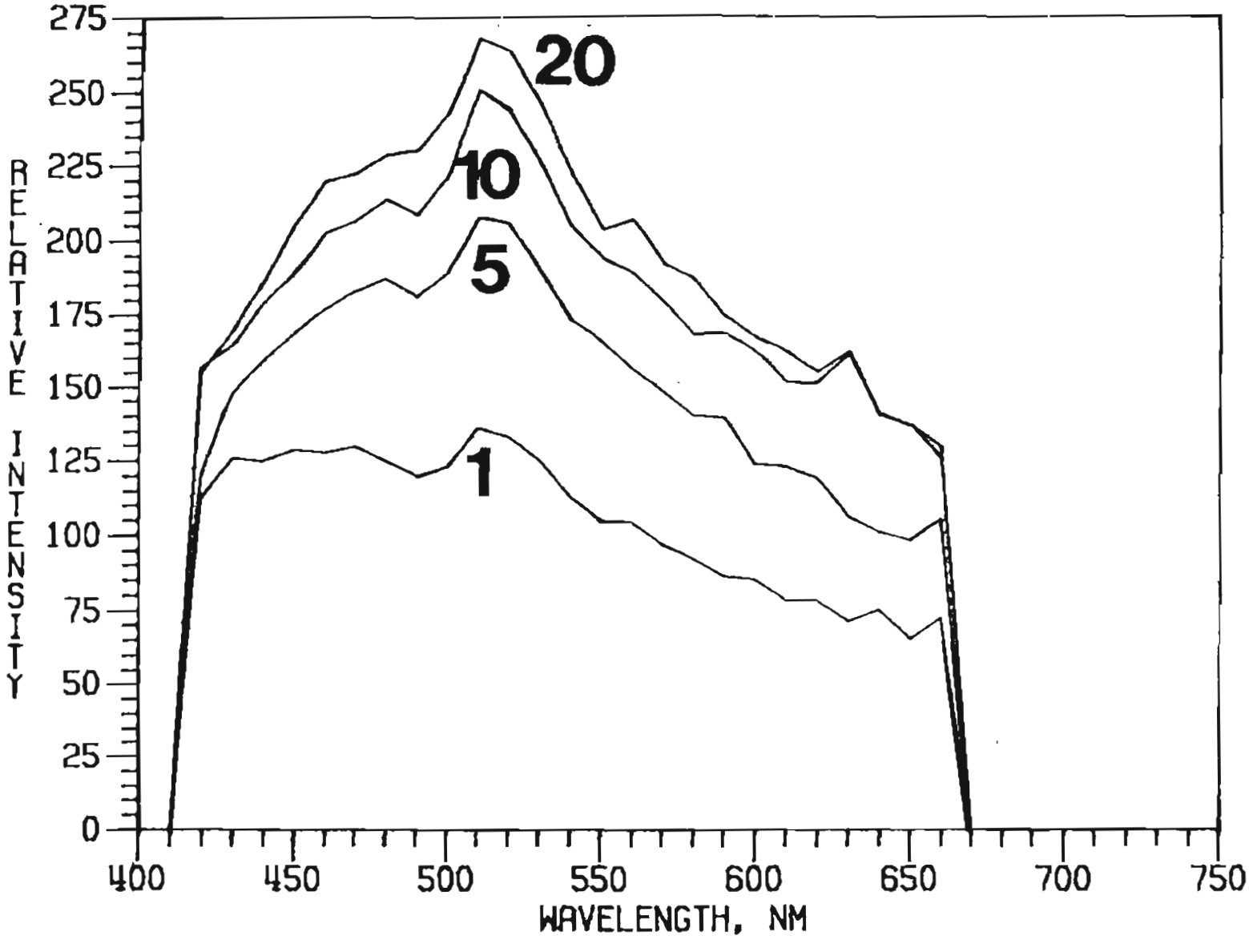

Figure 20. Fluorescence spectra of ulminite in HZA.
(Irradiated for 1, 5, 10 and 20 min)

Table 6 Characteristics of Fluorescent Ulminite Spectra

	Irradiation Time (minutes)			
	1	5	10	20
Location of I_{max}, nm	510	510	510	510
Red/Green Quotient	.523	.521	.617	.565
Area of Blue, %	42.5	39.7	38.0	38.2
Area of Green, %	30.9	32.7	32.3	32.9
Area of Yellow, %	18.6	19.7	20.9	20.6
Area of Red, %	8.0	8.0	8.8	8.3
Area of $< I_{max}$, %	42.5	39.7	38.0	38.2
Area of $> I_{max}$, %	52.3	54.9	56.6	56.3

The relative intensity of the fluorescence spectrum was found to increase dramatically during the first 5 minutes of irradiation. Above a period of 20 minutes no further increase in intensity was observed. The location of maximum intensity remained unaffected by the length of irradiation. Finally, there is a slight red shift which is most prominent during the first 10 minutes.

No fluorescent macerals were observed in the liquefaction residues. The HZA coal is extremely reactive; over 75% of the coal was converted during short contact (3 min) thermal hydrogenation at 425°C. This loss in fluorescence correlates with the loss of aromatic skeletal vibrations in the infrared spectra of the hexane-insolubles. The fluorescence of the ulminite in HZA is presumably due to the presence of substituted aromatics such as:

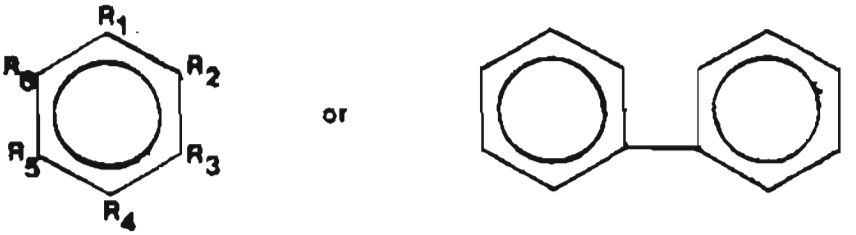

where R_n is H or a polar functional group.

If aromatic systems such as pyrene were responsible for the observed fluorescence, a synergistic affect could be realized by blending this coal with poor liquefying coals, such as UA-107. Such systems are capable of shuttling hydrogen via catalytic hydrogenation and as such are better H donors than tetralin (Derbyshire et al., 1981). If any synergistic effect is to be realized using this reactive coal, then it would stem from the generated products acting as plasticizers. These could hasten the solubilization of the less reactive coal and minimize the formation of products due to retrogressive reactions.

b) Inertinites

Sample UA-139, a coal from Cape Beaufort, was selected for evaluating the behavior of inert macerals. This coal consists of 40% inertinites most of which are semifusinites. Float-sink techniques were used to further concentrate this maceral group.

The distribution of maceral groups are listed in Table 7. (The specific macerals are listed in Table D.) Despite the relatively large particle size of the sample being washed, the inerts were concentrated in the heavier fractions. Macrinites tended to be concentrated in the 1.4 to 1.6 specific gravity fraction, and fusinite

was concentrated in the 1.6 specific gravity sink fraction. Semifusinite was equally distributed in both of these fractions. Most of the mineral matter was concentrated in the 1.6 sink. This fraction contains over 66% mineral matter.

Table 7 Maceral Groups in the Densimetric Fractions from Cape Beaufort Coal, UA-139

65 mesh by 0

Product	Vitrinite	Exinite	Inertinite
1.3-1.4	87	7	6
1.4-1.6	56	2	42
1.6-Sink	48	1	51

The specific gravity washing products were liquefied as previously described. The conversion yields for these fractions are given in Table 8. The 1.3-1.4 fraction is composed of essentially vitrinites and liptinites and was found to be readily converted.

Table 8 Conversion of Densimetric Fractions from Sample UA-139 (runs conducted at 425°C for 30 min, 600 psig H_2)

Product	Conversion to THF Solubles Plus Gases, % daf
1.3-1.4	87.50
1.4-1.6	64.98
1.6-Sink	63.09

As expected, the inertinite enriched 1.4-1.6 and 1.6-sink fractions are considerably less reactive than the 1.3-1.4 fraction. However, these yields are higher than can be accounted for by the volume of reactive macerals in these samples. We assume that some of the semifusinite has been converted to THF solubles. An attempt was made

to verify this. Polished mounts of the residues were optically examined. However, extensive comminution of the particles made identification of the residual inertinites meaningless.

The 1.6 sink fraction was found to be nearly as reactive as 1.4-1.6 fraction, despite the former fraction having a higher concentration of inertinites and in particular fusinite. Most likely the high concentration of mineral matter is responsible for the higher than anticipated yield. Two different effects are suggested. One is that the mineral matter may exhibit some catalytic activity. Examination of infrared spectrum of the sample indicated that kaolinite is the predominant mineral species present. The catalytic affect of kaolinite in coal hydrogenation has been well documented (Mukherjee and Chowdhury, 1976). A second influence is that the mineral matter may act as a diluent. As such, it could prevent or inhibit retrogressive reactions which would result in the formation of high molecular weight products or even result in a reduction in conversion. From this study it is not possible to discern which effect the mineral matter exerts.

ROLE OF MINERAL MATTER IN LIQUEFACTION STUDIES

Pyrite appears to play an important role in the hydrogenation of spent donor solvent or in some other catalytic capacity as itself, as pyrrhotite derived from it or as some intermediate iron sulfide. However, the catalytic advantages of pyrite or generated H_2S are denied due to the low sulfur content of Alaskan coals. With the exception of sample DH 1-5, which has a sulfur content of 3.23% daf,

the average sulfur content of the coals in the sample set is below 0.7%. Even for this high suflur coal, no noticeable differences in its product distribution or conversion yield are apparent.

In order to investigate the existence of other minerals or inorganics with catalytic activity, the distribution of inorganic elements in these coals was examined. The results of ash analysis of the coals are presented in Table 9, with the elements expressed on a dry coal basis. It is noteworthy that Ca is present in the Nenana coals (UA-119, UA-129, UA-130, 2UCM-11) in up to 2 wt. % of the coal. Much of this Ca is present as a carboxylate salt, part of which ultimately ends up as vaterite in the liquefaction products. Perry and Allardice (1983) suggested that carboxylates can have a stabilizing influence on the thermal decomposition of the coal. If so, then this influence may also diminish the tendency for condensation reactions to occur. Experimentation was conducted to establish the validity of this scenario.

For this study, a reactive subbituminous coal (2UCM-11) and a considerably less reactive inertinite rich bituminous coal (CSB-13) were used. The influences of cations on the liquefaction behavior of these coals was examined at three loadings: ammonium acetate washed, ammonium acetate washed followed by calcium loading, and the raw coal. There is a marked increase in the 30 min conversion of both coals with increase in Ca loading, as shown in Figure 21. The linearity of the data in these plots is reduced slightly due to the presence of other cations in the raw coal, particularly Mg and Na, which are not accounted for in the middle points.

Table 9. Distribution of Inorganic Elements in Coal*

Sample	Si	Fe	Ca	Mg	Mn	Na	Ti	Al	K	Ba	Sr
UA-148	131000	8900	4930	1830	140	270	1850	63600	6850	621	200
DH 1-2	43900	4830	11000	1890	100	120	1090	37200	256	405	230
DH 1-4	12000	5830	11500	2140	75	66	536	11100	449	678	300
DH 1-5	55700	14000	9200	1930	81	160	1700	43300	1270	752	250
DH 1-6	126000	8890	9400	4300	85	330	3030	77200	5860	586	220
CS 41730	33700	10400	15900	3050	310	97	918	18500	1260	1570	110
CS 41735	13300	9210	9810	1690	98	62	463	12700	621	698	72
UA-107	62600	6980	4100	1740	89	510	1580	34500	2350	788	260
UA-119	12800	4960	20700	2110	63	54	398	7760	268	521	200
UA-129	61800	5740	20200	2620	120	280	1350	30100	1640	1360	490
UA-130	3020	4820	19200	2070	110	40	108	3530	49	595	260
2UCM-11	10000	6450	15900	1960	270	67	353	7940	420	392	210
UA-139	122000	4770	9790	3450	65	6600	1580	47600	2590	1260	140
SS 67-1	2050	3460	2990	2240	15	500	50	1150	26	208	49
SS 67-2	5680	2020	12100	5480	9	1200	499	9010	211	461	300
SS 67-3	11600	1630	2410	1770	7	1100	344	11600	306	685	230
CSB 13	9430	3220	15300	2160	14	4880	837	10600	354	1960	480

* Expressed on PPM dry coal basis

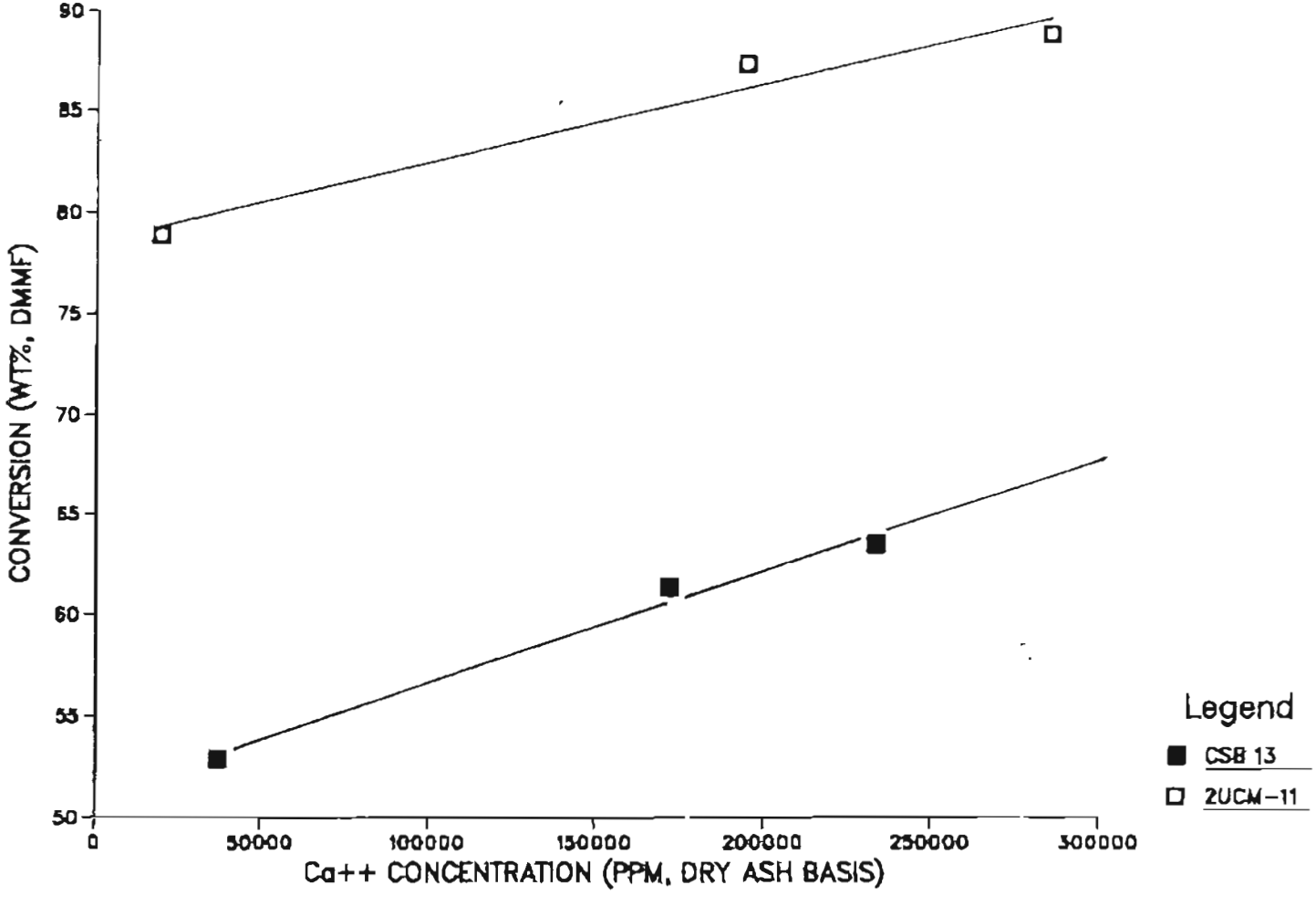

Figure 21. Effect of calcium cations on conversion.

We infer that 2UCM-11 experiences a localized hydrogen deficiency due to the high concentration of labile bonds present in its matrix. Furthermore, CSB-13 is less reactive, presumably fewer bonds are broken or the linkages are less labile. This results in a longer period of time needed to break down the matrix and solubilize the coal fragments. In both of these cases, the donor solvent can be diffusion limited. The presence of cations appears to reduce the extent of retrogressive reactions resulting from this condition. For coals endowed with sufficient quantities of donatable hydrogen, the presence of cations may tend to inhibit product generation and have an opposite effect to that shown here. Such an effect has been noted by Whitehurst et al. (1980) and Winans et al. (1983) to occur during short contact liquefaction.

SUMMARY AND CONCLUSIONS

This report has discussed the behavior of 19 Alaskan coals varying in both rank and maceral composition. The lignite and subbituminous coals from Little Tonzona, Nenana, Beluga and Yukon Flats coal fields were very reactive under the liquefaction conditions employed. They produced primarily low molecular weight type products. The inertinite-rich coals from Northern Alaska and Chicago Creek were considerably less reactive and produced a distribution of products. The bituminous coal from the Matanuska coal field gave poor conversion yields, most of which were preasphaltenes. This behavior is attributed to the high concentration of pseudovitrinite in this coal rather than oxidative affects.

The HZA coal was found to be the most reactive coal examined and to exhibit some rather unusual properties. For these reasons it was examined in greater detail. Its infrared spectrum contains many of the features found in spectra of lignins. The major spectral differences between the HZA coal and other coals were lost upon conversion. Coinciding with these changes was the loss in the fluorescence of the ulminite in this coal. We inferred that this fluorescence is due to the presence of substituted aromatics.

Densimetric fractionations of UA-139 further concentrated the inertinites contained in this coal. Higher conversions were obtained than could be accounted for by the concentration of vitrinite + exinites. The low reflectance semifusinite are assumed to be partially converted.

The role of the cations and mineral matter during liquefaction were found to differ yet have similar effects on increasing conversion yields. High concentrations of mineral matter acted as a diluent and hindered the occurrence of retrogressive reactions. Cations influence the thermal decomposition of coal. In cases such as reported here, where on a local level hydrogen capping reactions cannot compete with condensation reactions, cations reduce the tendency for the latter to occur.

REFERENCES

Barker, J. (1981), Coal and Uranium Investigation of the Yukon Flats Cenozoic Basin, Open File Report, prepared for U.S. Department of Interior, Report No. 140-81.

Blom, L. (1960), Analytical Methods in Coal Chemistry, Ph.D. Thesis, Technische Hogesschool of Delft, Netherlands.

Cronauer, D.C. and Ruberto, R.G. (1977), Investigation of mechanism of reactions involving oxygen-containing compounds in coal, Report prepared for Electric Power Research Institute, Report No. AF-422.

Derbyshire, F.J. (1982), personal communication.

Derbyshire, F.J. and Whitehurst, D.D. (1981), Study of coal conversion in polycondensed aromatic compounds, Fuel, 60, 655-662.

Durie, R.A. (1980), The characteristics of Australian coals and their implications in coal liquefaction, in Coal Liquefaction Fundamentals, ed. D. Dwayne Whitehurst, ACS Symposium Series No. 139, Amer. Soc., p. 53-73.

Epperly, W.R. (1980), Annual Technical Progress Report FE-2893-53 from Exxon Research and Engineering Company to U.S. Department of Energy.

Given, P.H. (1984), An Essay on the Organic Geochemistry of Coal, in Coal Science, Volume 3, ed. M.L. Gorbaty, J.W. Larsen and I. Wender, Academic Press, Inc., San Diego, Calif., p. 63-252.

Given, P.H., Cronauer, D.C., Spackman, W., Lovell, H.L., Davis, A. and Biswas, B. (1975a), Dependence of coal liquefaction behavior on coal characteristics. 1. Vitrinite-rich samples, Fuel, 54, 34-39.

Given, P.H., Cronauer, D.C., Spackman, W., Lovell, H.L., Davis, A. and Biswas, B. (1975b), Dependence of coal liquefaction behavior on coal characteristics. 2. Role of petrographic composition, Fuel, 54, 40-49.

Given, P.H., Spackman, W., Davis, A. and Jenkins, R.G. (1980), Some proved and unproved effects of coal geochemistry on liquefaction behavior with emphasis on U.S. coals, in Coal Liquefaction Fundamentals, ed. D. Dwayne Whitehurst, ACS Symposium Series No. 139, Amer. Chem. Soc., p. 3-34.

Given, P.H., Spackman, W., Davis, A., Walker, P.L., Lovell, H.L., Coleman, M.M. and Painter, P.C. (1982), The relation of coal characteristics to liquefaction behavior, Final Technical Report for the Period July 1976 to February 1981, prepared for U.S. Department of Energy, Report No. PE-2494-FR-3.

Given, P.H. and Derbyshire, F.J. (1985), The Mobile Phase in Coals: Its Nature and Modes of Release, Quarterly Progress Report, prepared for U.S. Dept. of Energy, Report No. DOE-PE-60811-6.

Gray, D., Barrass, G., Jezko, J. and Kershaw, J.R. (1980), South African coals and their behavior during liquefaction, in Coal Liquefaction Fundamentals, ed. D. Dwayne Whitehurst, ACS Symposium Series No. 139, Amer. Chem. Soc. p. 35-51.

Hergert, H.L. (1971), Infrared Spectra. in Lignins: Occurrence. Formation. Structure and Reactions, ed. K.V. Sarkanen and C.H. Ludwig, Wiley-Interscience, New York, p. 267-297.

Morgan, M.E., Jenkins, R.G. and Walker, P.L. (1981), Inorganic Constituents in American lignites, Fuel, 60, 189-193.

Mukherjee, D.K. and Choudhury, P.B. (1976), Catalytic effect of mineral matter constituents in a North Assam coal on hydrogenation, Fuel, 55, 4-8.

Painter, P.C., Coleman, M.M., Snyder, R.W., Mahajan, O., Komatsu, M. and Walker, P.L. (1981), Low Temperature Air Oxidation of Coking Coals: Fourier Transform Infrared Studies, Applied Spectroscopy, 35, 106-110.

Painter, P.C., Starsinic, M. and Coleman, M.M. (1985), Determination of Functional Groups in Coal by Fourier Transform Interferometry, Fourier Transform Infrared Spectroscopy, 4, 169-241.

Perry, G.J. and Allardice, D.J. (1983), The Characteristics of Victorian Brown Coal in Relation to Hydrogenation performance, in Proc. International Conference on Coal Science, Pittsburgh, p. 44-47.

Rhoads, C. (1985), The contribution of Plant Polymers to Coal Formation, Ph.D. Thesis, The Pennsylvania State University, 181 pp.

Rao, P.D. and Wolff, E.N. (1980), Characterization and Evaluation of Washability of Alaskan Coals, Final Technical Report for Phase II for the period July 1977 - February 1979, prepared for U.S. Department of Energy, Report No. DOE/ET/13350-T2.

Rao, P.D. and Wolff, E.N. (1982), Characterization and Evaluation of Washability of Alaskan Coals, Final Technical Report for Phase III for the period March 1979 - January 1982, prepared for U.S. Department of Energy, Report No. DOE/ET/13350-T6.

Rao, P.D. and Smith, J. (1983), Petrology of Cretaceous coals from northern Alaska, Final report submitted to U.S. Dept. of Energy, Project DOE-DE-FG22-80PC30237.

Schaff, R.G. (1983), Coal Resources of Alaska, Division of Geological and Geophysical Survey, Information Circular 17, 9 pp.

Suhr, N.H. and Gong, H. (1983), Some Procedures for the Chemical and Mineralogical Analysis of Coals, Final Report - Part 3, prepared for U.S. Dept. of Energy, report no. DOE-30013-F3.

Szladow, A.J. (1979), Some aspects of the mechanism and kinetics of coal liquefaction, Ph.D. Thesis, Pennsylvania State University.

Walker, P.L., Spackman, W., Given, P.H., Davis, A., Jenkins, R.G. and Painter, P.C. (1980), Characterization of mineral matter in coals and coal liquefaction residues, Annual Report AP-1634 from Pennsylvania State University to Electric Power Research Institute.

Whitehurst, D.D., Farcasiu, M., Mitchell, T.O. and Dickert, J.J. (1979), The Nature and Origin of Asphaltenes in Processed Coals: Chemistry and Mechanisms of Coal Conversion to Clean Fuel, Report prepared for Electric Power Research Institute, AF-1298.

Whitehurst, D.D., Mitchell, T.O. and Fracasiu, M. (1980), Coal Liquefaction, Academic Press, N.Y., 378 pp.

Winans, R.E., King, H.H., McBeth, R.L. and Botto, R.B. (1983), Preprints, Amer. Chem. Div., 28(5), 8-16.

Yarzab, R.F., Given, P.H. and Abdel-Baset, Z. (1979), Hydroxyl contents of coals: new data and statistical analyses, Geochem. et Cosmochim. Acta, 43, 281-287.

Yarzab, R.F., Given, P.H., Spackman, W. and Davis, A. (1980), Dependence of coal liquefaction behavior on coal characteristics. 4. Cluster analyses for characterization of 104 coals, Fuel, 59, 81-92.

Youtcheff, J.S. (1983), Contributions to the understanding of the phenomenology of coal liquefaction, Ph.D. Thesis, Pennsylvania State University, 245 pp.

Appendix A

Coal Characteristics

TABLE A
PROXIMATE AND ULTIMATE ANALYSES OF COALS

Sample Numbers	Basis*	Moisture %	Volatile Matter,%	Fixed Carbon,%	Ash %	Heating Value BTU/LB	C,%	H,%	N,%	O,%	Sulfur Total
UA 148	1	21.21	25.64	24.38	28.77	5545.	33.38	5.18	0.42	31.86	0.39
	2	1.47	32.06	30.49	35.98	6934.	41.74	3.68	0.52	17.59	0.49
	3		32.54	30.94	36.52	7037.	42.36	3.57	0.53	16.53	0.50
	4		51.25	48.75		11086.	66.73	5.62	0.83	26.03	0.78
DH 1-2	1	36.76	23.93	29.06	10.25	6384.	38.37	6.69	0.78	43.35	0.56
	2	3.74	36.42	44.24	15.60	9718.	58.40	4.34	1.19	19.61	0.86
	3		37.84	45.96	16.21	10096.	60.67	4.07	1.24	16.92	0.89
	4		45.15	54.85		12048.	72.40	4.86	1.48	20.19	1.07
DH 1-4	1	38.12	25.16	31.72	4.99	6884.	41.09	6.94	0.77	45.39	0.83
	2	4.09	39.00	49.17	7.74	10670.	63.68	4.60	1.19	21.51	1.28
	3		40.66	51.27	8.07	11125.	66.40	4.32	1.24	18.64	1.33
	4		44.23	55.77		12102.	72.22	4.70	1.35	20.28	1.45
DH 1-5	1	35.96	24.18	26.49	13.38	5906.	34.97	6.59	0.48	42.95	1.64
	2	3.48	36.44	39.92	20.16	8902.	52.70	4.26	0.72	19.69	2.47
	3		37.75	41.36	20.89	9223.	54.60	4.01	0.75	17.20	2.56
	4		47.72	52.28		11658.	69.02	5.07	0.94	21.74	3.23

*1 As Received
2 Air Dried Moisture
3 Moisture Free
4 Moisture and Ash Free

TABLE A (continued)
PROXIMATE AND ULTIMATE ANALYSES OF COALS

Sample Numbers	Basis*	Moisture %	Volatile Matter,%	Fixed Carbon,%	Ash %	Heating Value BTU/LB	C,%	H,%	N,%	O,%	Sulfur Total
DH 1-6	1	33.16	19.79	22.59	24.46	4960.	29.69	5.82	0.69	38.58	0.76
	2	2.22	28.95	33.05	35.78	7256.	43.43	3.34	1.01	15.33	1.11
	3		29.61	33.80	36.59	7421.	44.42	3.16	1.03	13.66	1.14
	4		46.69	53.31		11703.	70.05	4.99	1.63	21.55	1.79
CS 41730	1										
	2	11.38	45.58	31.42	11.62	8706.	51.39	5.46	0.58	30.25	0.70
	3		51.43	35.45	13.11	9024.	57.99	4.72	0.65	22.73	0.79
	4		59.19	40.81		11306.	66.74	5.44	0.75	26.16	0.91
CS 41735	1										
	2	12.46	44.02	35.36	7.36	9105.	53.39	5.42	0.59	33.06	0.18
	3		51.02	40.39	8.41	10401.	60.99	4.60	0.67	25.12	0.21
	4		55.90	44.10		11356.	66.59	5.02	0.74	27.43	0.22
UA 107	1	1.44	27.78	54.59	16.18	12493.	70.45	4.98	1.67	6.28	0.44
	2	0.18	28.14	55.29	16.39	12653.	71.35	4.90	1.69	5.22	0.45
	3		28.19	55.39	16.42	12676.	71.48	4.89	1.69	5.07	0.45
	4		33.73	66.27		15166.	85.52	5.85	2.03	6.07	0.54

*1 As Received
2 Air Dried Moisture
3 Moisture Free
4 Moisture and Ash Free

TABLE A (continued)
PROXIMATE AND ULTIMATE ANALYSES OF COALS

Sample Numbers	Basis*	Moisture %	Volatile Matter,%	Fixed Carbon,%	Ash %	Heating Value BTU/LB	C,%	H,%	N,%	O,%	Sulfur Total
UA 119	1	28.36	34.65	31.74	5.25	7699.	45.68	6.62	0.54	41.74	0.18
	2	3.69	46.58	42.67	7.06	10350.	61.41	5.04	0.72	25.53	0.24
	3		48.36	44.30	7.33	10747.	63.76	4.80	0.75	23.11	0.25
	4		52.19	47.81		11597.	68.81	5.18	0.81	24.93	0.27
UA 129	1	24.43	32.51	28.97	14.09	7061.	41.91	6.04	0.55	37.24	0.17
	2	3.16	41.66	37.13	18.05	9048.	53.71	4.59	0.70	22.73	0.22
	3		43.02	38.34	18.64	9343.	55.46	4.37	0.72	20.57	0.23
	4		52.87	47.13		11484.	68.17	5.38	0.89	25.29	0.28
UA 130	1	29.45	34.56	32.18	3.82	7859.	46.30	6.79	0.52	42.44	0.12
	2	2.74	47.64	44.36	5.26	10035.	63.83	5.13	0.72	24.89	0.17
	3		48.90	45.61	5.41	11140.	65.63	4.96	0.74	23.09	0.17
	4		51.78	48.22		11777.	69.38	5.24	0.78	24.41	0.18
2UCM-11	1	27.59	35.03	31.46	5.91	7882.	45.83	6.49	0.51	41.01	0.26
	2	4.72	46.10	41.40	7.78	10372.	60.30	5.00	0.67	25.91	0.34
	3		48.38	43.45	8.17	10886.	63.29	4.69	0.70	22.79	0.36
	4		52.69	47.31		11854.	68.91	5.11	0.77	24.81	0.39

*1 As Received
2 Air Dried Moisture
3 Moisture Free
4 Moisture and Ash Free

TABLE A (continued)
PROXIMATE AND ULTIMATE ANALYSES OF COALS

Sample Numbers	Basis*	Moisture %	Volatile Matter,%	Fixed Carbon,%	Ash %	Heating Value BTU/LB	C,%	H,%	N,%	O,%	Sulfur Total
CSB 13	1	16.46	25.58	50.53	7.43	9274.	57.65	4.95	0.86	28.96	0.15
	2	3.06	29.68	58.64	8.62	10762.	66.90	3.95	1.00	19.36	0.17
	3		30.62	60.49	8.89	11102.	69.01	3.72	1.03	17.17	0.18
	4		33.61	66.39		12185.	75.75	4.08	1.13	18.84	0.19
HZ A	1										
	2	0.48	54.92	41.95	2.65	10574.	61.42	5.58	0.32	29.11	0.92
	3		55.18	42.15	2.66	10625.	61.72	5.55	0.32	28.82	0.92
	4		56.69	43.31		10916.	63.40	5.70	0.33	29.61	0.95
HZ E1	1										
	2	10.54	29.46	22.35	37.65	5867.	35.49	3.97	0.43	21.76	0.70
	3		32.93	24.98	42.09	6558.	39.67	3.12	0.48	13.86	0.78
	4		56.86	43.14		11324.	68.50	5.39	0.83	23.93	1.35

*1 As Received
2 Air Dried Moisture
3 Moisture Free
4 Moisture and Ash Free

TABLE B
VITRINITE REFLECTANCE
DATA

Sample	Classes											
	V_1	V_2	V_3	V_4	V_5	V_6	V_7	V_8	V_9	V_{10}	V_{11}	$\bar{R}_{max}$
UA 148	76	18	6									.19
DH 1-2			44	52	4							.40
DH 1-4			45	54	1							.40
DH 1-5			38	59	3							.41
DH 1-6			13	83	4							.44
CS 41730	20	64	16									.24
CS 41735	52	36	12									.21
UA 107								8	54	36	2	.98
UA 119	52	40	4									.20
UA 129	2	46	48	4								.30
UA 130	6	52	36	6								.27
2UCM-11		82	18									.27
UA 139					34	56	10					.63
SS 67-1							78	22				.75
SS 67-2							48	52				.79
SS 67-3							20	42	38			.86
CSB 13					20	64	16					.64
HZ A	98	2										.16
HZ E1	72	28										.18

TABLE A (continued)
PROXIMATE AND ULTIMATE ANALYSES OF COALS

Sample Numbers	Basis*	Moisture %	Volatile Matter,%	Fixed Carbon,%	Ash %	Heating Value BTU/LB	C,%	H,%	N,%	O,%	Sulfur Total
UA 139	1	10.52	23.69	40.83	24.96	7876.	48.38	3.96	0.76	21.12	0.82
	2	1.56	26.06	44.92	27.46	8665.	53.22	3.24	0.84	14.34	0.90
	3		26.47	45.63	27.90	8802.	54.06	3.11	0.85	13.16	0.91
	4		36.71	63.29		12208.	74.98	4.32	1.18	18.25	1.27
SS 67-1	1										
	2	2.31	35.98	59.64	2.07	13731.	76.92	5.14	1.34	14.36	0.17
	3		36.83	61.05	2.12	14056.	78.74	5.00	1.37	12.60	0.17
	4		37.63	62.37		14360.	80.44	5.11	1.40	12.87	0.18
SS 67-2	1										
	2	2.40	32.12	59.71	5.77	12910.	73.61	4.81	1.22	14.42	0.17
	3		32.91	61.18	5.91	13227.	75.42	4.65	1.25	12.59	0.17
	4		34.98	65.02		14059.	80.16	4.95	1.33	13.38	0.19
SS 67-3	1										
	2	3.24	26.62	65.57	4.57	13178.	76.26	4.55	1.26	13.18	0.18
	3		27.51	67.77	4.72	13619.	78.81	4.33	1.30	10.65	0.19
	4		28.88	71.12		14294.	82.72	4.54	1.37	11.18	0.20

*1 As Received
2 Air Dried Moisture
3 Moisture Free
4 Moisture and Ash Free

TABLE C
MACERAL DISTRIBUTION*

SAMPLE	V	PV	Gel	Corpo	Sp	Rs	Exs	TCut	Cut	Sub	Lip	Alg	Flvit	Fus	SmF	M	GM	In	Scl
UA-148	75.1	1.6	1.6	5.2	3.0	3.2	2.0	0.6	0.4	0.2	1.2	--	--	0.2	3.0	1.1	1.4	.2	--
DH 1-2	44.4	0.5	1.2	2.6	4.8	3.4	0.8	0.6	0.4	--	2.0	--	--	2.8	17.2	3.2	1.1	14.8	0.2
DH 1-4	65.3	1.1	0.7	3.3	3.4	3.0	0.4	--	0.4	0.4	1.6	0.2	--	1.8	9.8	2.4	1.3	5.3	--
DH 1-5	59.3	0.7	0.2	1.7	3.8	4.4	1.8	--	0.8	--	2.0	--	--	1.4	11.9	1.4	1.4	9.2	--
DH 1-6	45.5	--	0.2	0.8	4.6	15.4	0.8	0.4	0.4	--	0.8	--	--	1.4	17.5	2.9	0.8	8.5	--
CS 41730	64.4	--	5.4	14.8	1.8	3.2	1.0	--	0.2	0.4	--	--	4.5	--	1.5	0.4	0.7	1.7	--
CS 41735	60.4	--	6.4	11.4	3.0	2.8	0.6	--	0.2	--	1.4	--	19.4	--	2.2	0.2	1.3	0.7	--
UA-107	67.0	18.2	--	--	1.0	8.4	0.8	0.6	--	--	0.8	0.2	--	--	1.4	0.5	--	--	1.1
UA-119	69.4	--	1.0	3.5	5.0	3.4	2.8	0.6	0.6	2.4	1.8	--	--	0.2	6.2	1.7	--	1.3	0.2
UA-129	63.7	1.4	0.2	1.1	9.4	4.6	1.4	--	--	0.8	6.4	--	--	0.5	6.8	1.2	0.5	1.9	0.2
UA-130	71.4	0.5	0.7	3.0	4.2	4.0	2.0	0.4	0.4	0.8	1.8	--	--	1.4	5.9	0.9	0.2	2.1	0.3
2UCM-11	77.8	--	1.3	4.5	4.2	2.0	1.2	--	--	0.8	1.6	--	--	0.1	4.6	0.7	0.2	0.9	0.2
UA-139	45.2	3.4	--	0.9	2.8	4.0	1.0	1.0	--	--	1.4	0.2	--	0.5	26.7	5.7	1.4	5.7	--

*Vol. %, mmf basis.

Key: V = vitrinite/humotelinite, PV = psuedovitrinite, Gel = gelocollinate + gelinite, Corpo = Corpocollinite + Corpohuminite, Sp = sporinite, Rs = resinite, Exs = exsudatinite, TCut = thick cutinite, Cut = cutinite, Sub = suberinite, Lip = other liptinites, Alg = alginite, Flvit = fluorescent vitrinite, Fus = fusinite, SmF = semifusinite, M = macrinite, GM = globular macrinite, In = inertodetrinite, Scl = sclerotinite.

TABLE C (continued)
MACERAL DISTRIBUTION*

SAMPLE	V	PV	Gel	Corpo	Sp	Rs	Exs	TCut	Cut	Sub	Lip	Alg	Flvit	Fus	SmF	M	GM	In	Scl
SS 67-1	74.6	13.2	2.8	1.8	1.6	--	--	--	--	--	--	0.6	--	--	4.2	0.4	--	0.8	--
SS 67-2	52.3	22.5	1.4	1.1	1.0	0.6	--	--	0.2	0.1	--	--	--	0.9	16.5	0.8	--	2.6	--
SS 67-3	54.0	4.9	2.0	2.1	1.3	0.3	--	0.1	0.2	--	--	0.1	--	0.6	27.2	2.1	1.5	3.5	.1
CSB 13	44.8	3.7	0.2	0.6	2.8	2.2	1.2	0.2	--	--	1.2	--	0.2	2.4	27.7	5.0	3.0	5.0	--
HZA	18.4	--	0.2	--	--	--	--	--	--	--	2.0	--	76.8	--	--	0.4	1.8	0.4	--
HZE1	70.2	--	0.7	1.4	3.2	4.4	0.4	--	--	--	2.0	--	--	0.2	5.2	1.3	1.1	9.9	--

*Vol. %, mmf basis.

Key: V = vitrinite/humotelinite, PV = psuedovitrinite, Gel = gelocollinate + gelinite, Corpo = Corpocollinite + Corpohuminite, Sp = sporinite, Rs = resinite, Exs = exsudatinite, TCut = thick cutinite, Cut = cutinite, Sub = suberinite, Lip = other liptinites, Alg = alginite, Flvit = fluorescent vitrinite, Fus = fusinite, SmF = semifusinite, M = macrinite, GM = globular macrinite, In = inertodetrinite, Scl = sclerotinite.

TABLE D
MACERAL DISTRIBUTION FOR UA-139
DENSIMETRIC FRACTIONS*

Product	V	PV	Gel	Corpo	Sp	Rs	Exs	TCut	Cut	Sub	Lip	Alg	Flvit	Fus	SmF	M	GM	In	Scl
1.4 Float	86.4	--	0.4	0.6	3.2	3.0	--	0.6	--	--	--	--	--	--	1.4	0.4	0.4	3.4	--
1.4-1.6	54.0	1.8	--	--	0.8	0.6	--	--	--	--	--	--	--	1.2	28.0	8.2	2.2	2.2	--
1.6 Sink	47.9	--	--	--	--	0.6	--	--	--	--	--	--	--	12.4	33.0	2.1	0.9	3.0	--

*Vol. %, mmf basis.

Key: V = vitrinite/humotelinite, PV = psuedovitrinite, Gel = gelocollinate + gelinite, Corpo = Corpocollinite + Corpohuminite, Sp = sporinite, Rs = resinite, Exs = exsudatinite, TCut = thick cutinite, Cut = cutinite, Sub = suberinite, Lip = other liptinites, Alg = alginite, Flvit = fluorescent vitrinite, Fus = fusinite, SmF = semifusinite, M = macrinite, GM = globular macrinite, In = inertodetrinite, Scl = sclerotinite.